Design and Performance of Limestone Drains to Increase pH and Remove Metals from Acidic Mine Drainage

Charles A. Cravotta III* **and George R. Watzlaf**[†]

*U.S. Geological Survey, New Cumberland, Pennsylvania 17070

[†]U.S. Department of Energy, National Energy Technology Laboratory, Pittsburgh, Pennsylvania 15236

Data on the construction characteristics and the composition of influent and effluent at 13 underground, limestone-filled drains in Pennsylvania and Maryland are reported to evaluate the design and performance of limestone drains for the attenuation of acidity and dissolved metals in acidic mine drainage. On the basis of the initial mass of limestone, dimensions of the drains, and average flow rates, the initial porosity and average detention time for each drain were computed. Calculated porosity ranged from 0.12 to 0.50 with corresponding detention times at average flow from 1.3 to 33 h. The effectiveness of treatment was dependent on influent chemistry, detention time, and limestone purity. At two sites where influent contained elevated dissolved Al (>5 mg/liter), drain performance declined rapidly; elsewhere the drains consistently produced near-neutral effluent, even when influent contained small concentrations of dissolved Fe^{3+} (<5 mg/liter). Rates of limestone dissolution computed on the basis of average long-term Ca ion flux normalized by initial mass and purity of limestone at each of the drains ranged from 0.008 to 0.079 $year^{-1}$. Data for alkalinity concentration and flux during 11-day closed-container tests using an initial mass of 4 kg crushed limestone and a solution volume of 2.3 liter yielded dissolution rate constants

that were comparable to these long-term field rates. An analytical method is proposed using closed-container test data to evaluate long-term performance (longevity) or to estimate the mass of limestone needed for a limestone treatment. This method considers flow rate, influent alkalinity, steady-state maximum alkalinity of effluent, and desired effluent alkalinity or detention time at a future time(s) and applies first-order rate laws for limestone dissolution (continuous) and production of alkalinity (bounded).

I. INTRODUCTION

Acidic or abandoned mine drainage (AMD) degrades aquatic ecosystems and water supplies in coal- and metal-mining districts worldwide. The AMD typically contains elevated concentrations of dissolved and particulate iron (Fe) and dissolved sulfate (SO_4^{2-}) produced by the oxidation of pyrite (FeS_2) in coal and overburden exposed to atmospheric oxygen (O_2) (Rose and Cravotta, 1998; Nordstrom and Alpers, 1999). Half the acid produced by the stoichiometric oxidation of pyrite results from the oxidation of pyritic sulfur to SO_4^{2-} and the other half results from the oxidation of ferrous (Fe^{2+}) to ferric (Fe^{3+}) iron and its consequent precipitation as $Fe(OH)_3$ and related solids[1] (Bigham *et al.*, 1996; Cravotta *et al.*, 1999). Concentrations of manganese (Mn^{2+}), aluminum (Al^{3+}), and other solutes in AMD commonly are elevated due to aggressive dissolution of carbonate, oxide, and aluminosilicate minerals by acidic water along paths downflow from oxidizing pyrite (Cravotta, 1994; Blowes and Ptacek, 1994).

AMD commonly develops where the carbonate minerals, calcite ($CaCO_3$) and dolomite [$CaMg(CO_3)_2$], are absent or deficient relative to pyrite in coal overburden (Brady *et al.*, 1994, 1998). Dissolution of calcite, which is the principal component of limestone, can neutralize acidity and increase pH and concentrations of alkalinity ($CO_3^{2-} + HCO_3^- + OH^-$) and calcium ($Ca^{2+}$) in mine water (Cravotta *et al.*, 1999). The overall rate of calcite dissolution generally decreases with increased pH, decreased partial pressure of carbon dioxide (P_{CO_2}), and increased activities of Ca^{2+}, bicarbonate (HCO_3^-), and carbonate (CO_3^{2-}) near the calcite surface (Plummer *et al.*, 1979; Morse, 1983; Arakaki and Mucci, 1995).

Acidity and metals can be removed from AMD through various passive treatment systems that increase pH and alkalinity (Hedin *et al.*, 1994a;

[1]Hereafter, $Fe(OH)_3$ indicates the hydrous Fe-oxide and -sulfate compounds that together form ochres in AMD environments, including $Fe(OH)_3$ or ferrihydrite (nominally $Fe_5HO_8 \cdot 4H_2O$), goethite (α–FeOOH), schwertmannite [$Fe_8O_8(OH)_6SO_4$], and jarosite [$(H,K,Na)Fe_3(SO_4)_2(OH)_6$] (Taylor and Schwertmann, 1978; Ferris *et al.*, 1989; Murad *et al.*, 1994; Bigham *et al.*, 1996).

Skousen *et al.*, 1998). Many of these systems utilize crushed limestone in packed beds in series with settling ponds or wetlands. For example, anoxic limestone drains (ALDs) are particularly effective for the generation of alkalinity (Turner and McCoy, 1990; Brodie *et al.*, 1991; Hedin and Watzlaf, 1994; Hedin *et al.*, 1994b; Watzlaf *et al.*, 2000a,b). Typically, for an ALD, crushed limestone of uniform size is placed in a buried bed(s) that intercepts net acidic (acidity > alkalinity) AMD before its exposure to atmospheric O_2. Excluding O_2 from contact with the mine water in an ALD minimizes the potential for oxidation of Fe^{2+} and precipitation of $Fe(OH)_3$.

The precipitation of $Fe(OH)_3$ and various other hydroxide and/or sulfate compounds of Fe^{3+}, Al^{3+}, and, possibly, Ca^{2+} and SO_4^{2-} within a bed of crushed limestone can "armor" the limestone surface (strong adhesion and complete pacification by encrustation), decreasing the rate and extent of limestone dissolution and alkalinity production (Watzlaf *et al.*, 1994; Hedin and Watzlaf, 1994; Aschenbach, 1995; Robbins *et al.*, 1999). Furthermore, the accumulation of precipitated compounds can decrease the porosity and permeability of the packed bed (Watzlaf *et al.*, 1994, 2000a,b; Robbins *et al.*, 1996). Hence, design criteria for ALDs as proposed by Hedin *et al.* (1994a) and Hedin and Watzlaf (1994) generally are conservative with respect to influent chemistry (requirement of <1 mg/liter of dissolved O_2, Fe^{3+}, or Al^{3+}) and sizing (prolonged detention time) to ensure "maximum" alkalinity production over the life of an ALD.

Although most ALDs have been constructed as horizontal flooded systems, where a greater head at the inflow than outflow maintains the hydraulic gradient, some systems have been designed for vertical flow (upward or downward). Continuous inundation and detention of CO_2 within an ALD can enhance calcite dissolution and alkalinity production. By this mechanism, a greater quantity of alkalinity can be generated in an ALD compared to systems such as limestone channels (Ziemkiewicz *et al.*, 1997) or diversion wells (Arnold, 1991; Cram, 1996) that are open to the atmosphere. After treatment by an ALD, effluent is typically routed through ponds and/or wetlands where exposure to the atmosphere facilitates Fe^{2+} oxidation and the precipitation and settling of solid $Fe(OH)_3$.

Stringent requirements for low concentrations of O_2, Fe^{3+}, and Al^{3+} in the influent AMD make ALDs inappropriate for the treatment of oxic or highly mineralized water, which commonly occurs in mined areas. For example, of 140 AMD samples collected in 1999 from bituminous and anthracite coal mines in Pennsylvania (Cravotta *et al.*, 2001), only 17% were net acidic *and* had <1 mg/liter of dissolved O_2, Fe^{3+}, and Al^{3+}. Thus, ALDs could be appropriate for AMD treatment at a minority of the 140 sites, provided the dissolved O_2, Fe^{3+}, and Al^{3+} concentrations remain at low levels *and* resources and space are available for construction of the treatment

system. However, for the majority of these discharges that do not meet criteria for an ALD, variations of the basic ALD design could be appropriate. One alternative uses pretreatment through a compost bed to decrease concentrations of dissolved O_2, Fe^{3+}, and Al^{3+} in the mine water to acceptable levels before routing the water through a limestone bed (Kepler and McCleary, 1994; Watzlaf *et al.*, 2000b). Nevertheless, short-term laboratory studies (<2 years) indicate that limestone alone can be as effective as this layered system for the neutralization of mine water containing dissolved O_2 and low-to-moderate concentrations of Fe^{3+} and Al^{3+} (<1–20 mg/liter) (Watzlaf, 1997; Sterner *et al.*, 1998). This variation on the ALD design is essentially an oxic limestone drain (OLD). In an enclosed OLD, oxidation and hydrolysis reactions will not be prevented but must be managed (Cravotta and Trahan, 1999). Despite the potential for armoring and clogging, hydrous oxides can be effective for the sorption of dissolved Mn^{2+} and trace metals (e.g., Kooner, 1993; Coston *et al.*, 1995; Webster *et al.*, 1998; Cravotta and Trahan, 1999). Precipitation of Mn oxides is possible after most dissolved Fe has been precipitated (Watzlaf, 1997; Cravotta and Trahan, 1999). If sufficiently rapid flow rates can be attained, the solid hydrolysis products may be transported through the OLD; however, consensus on design criteria for OLDs generally has not been reached.

This chapter evaluates the performance of limestone drains for the treatment of acidic, metal-contaminated water. Data on the basic design and chemical compositions of influent and effluent of 13 limestone drains that were constructed to treat discharges from abandoned coal mines in Pennsylvania and Maryland are evaluated with respect to flow rate, detention time, limestone dissolution rate, and long-term prospects for effectiveness. Criteria and methods for sizing and evaluation of limestone drains and general considerations for treatment of AMD containing dissolved O_2 and metals are presented.

II. SITE DESCRIPTIONS AND METHODS OF DATA COLLECTION

A. Description of Limestone Drains

The 13 limestone drains in Pennsylvania and Maryland considered for this study had varying designs reflecting site-specific treatment requirements and space availability. Detailed engineering documentation was not available; however, general descriptions of the drains were reported previously (Watzlaf *et al.*, 2000a,b; Cravotta and Trahan, 1999; Cravotta and Weitzel,

2001). Most drains were constructed as horizontal, buried limestone beds with an elongated form. Untreated inflow was intercepted within the trench or was piped into the drain. If possible, trenches were excavated in clay or liners were installed to prevent leakage. Generally, the outflow pipe from each of the flooded drains was extended to a level above the top of the limestone to ensure continuous inundation of the limestone and to minimize airflow into the drains. Additional information is provided here and in Table I.

Howe Bridge 1. Discharge from an abandoned well is captured and piped to the limestone drain. Influent water is sampled via a well prior to contact with limestone. Four sampling wells are spaced evenly along the length of the drain.

Howe Bridge 2. Discharge from another abandoned well is treated in an S-shaped limestone drain. Influent water is sampled via a well as the water flows into the limestone drain. Two sampling wells are along the length of the drain.

Elklick. Water from an abandoned borehole is collected in a bed ($7.0 \times 1.8 \times 0.9$ m) of crushed, low-pyrite sandstone at the head of the limestone drain. Influent water is sampled at a well in this sandstone. Three sampling wells are spaced equally along the length of the drain.

Jennings. The limestone drain treats an abandoned underground mine discharge that is collected in an bed of inert river gravel and piped to the system. Influent water is sampled via a sampling well prior to contact with limestone. The limestone drain consists of a series of six buried limestone-filled cells.

Morrison. Seepage is intercepted at the toe of the spoil of a reclaimed surface mine. An adjacent seep, similar in quality to the preconstruction water, is used to represent influent water quality. Three sampling wells are along the length of the limestone drain.

Filson-R and Filson-L. Seepage is intercepted at the toe of the spoil. A seep, between limestone drains, is similar in quality to the preconstruction raw water and is used to represent influent water quality.

Schnepp, REM-R, and REM-L. At each site, a limestone drain was constructed downgradient from collapsed underground mine entrances. Influent water quality is based on historical data.

Orchard. Three parallel limestone drains were constructed below a collapsed drift. Seepage from the drift was collected behind a wooden dam and then piped into the drains. Influent is accessible before contacting limestone. Valving at the inflow to each drain was used to control inflow rates. Access wells were installed at five locations along the length of each drain.

Table I

Initial Mass, Purity, Bulk Volume, Bulk Density, and Porosity of Crushed Limestone Used for Construction of 13 Limestone Drains in Pennsylvania and Maryland

Limestone drain site[a]	Year built[a] (t=0)	Mass of limestone, M_0 (tonne)[a]	Purity of limestone, X_{CaCO_3} (%)[a,b]	Size range limestone fragments (cm)[a]	Drain dimensions[a]			Bulk volume, V_B, (m^3)[c]	Bulk density, ρ_B, (kg/m^3)[d]	Porosity, ϕ (fractional units)[d]	Void ratio, $e = \phi/(1-\phi)$ (unitless)
					Length (m)	Width (m)	Depth (m)				
1. Howe Bridge 1	1991	455.0	82	5.1–7.6	36.6	6.1	1.2	267.9	1698	0.359	0.560
2. Howe Bridge 2	1993	132.0	82	5.1–7.6	13.7	4.6	0.9	56.7	2327	0.122	0.139
3. Elklick	1994	165.0	85	5.1–20.3	36.6	3.1	0.9	102.1	1616	0.390	0.640
4. Jennings	1993	365.0	90	15.2	228.0	1.0	1.0	228.0	1601	0.396	0.655
5. Morrison	1990	65.0	92	5.1–7.6	45.7	0.9	0.9	37.0	1756	0.337	0.509
6. Filson-R	1994	590.0	88	5.1–7.6	54.9	6.1	0.9	301.4	1958	0.261	0.354
7. Filson-L	1994	635.0	88	5.1–7.6	54.9	6.1	0.9	301.4	2107	0.205	0.258
8. Schnepp	1993	130.0	90	1.9–2.5	12.2	6.1	0.9	67.0	1941	0.268	0.365
9. REM-R	1992	125.0	82	7.6	16.8	6.1	0.9	95.1	1314	0.504	1.017
10. REM-L	1992	125.0	82	7.6	13.7	7.6	0.9	93.0	1344	0.493	0.972
11. Orchard	1995	38.1	97	6.0–10	73.2	2.4	0.8	16.7	2283	0.139	0.161

(*continues*)

Table I (*continued*)

Limestone drain site[a]	Year built[a] (t=0)	Mass of limestone, M_0 (tonne)[a]	Purity of limestone, X_{CaCO_3}, (%)[a,b]	Size range limestone fragments (cm)[a]	Drain dimensions[a] Length (m)	Width (m)	Depth (m)	Bulk volume, V_B, (m^3)[c]	Bulk density, ρ_B, (kg/m^3)[d]	Porosity, ϕ (fractional units)[d]	Void ratio, $e = \phi/(1-\phi)$ (unitless)
12. Buck Mountain	1997	320.0	92	6.0–10	48.8	1.9	1.9	176.2	1816	0.315	0.459
13. Hegins	2000	800.0	90	24–36	41.6	6.7	1.7	473.8	1688	0.363	0.570
Median									1756	0.337	0.509

[a]Data for year built, limestone mass, purity, size range, and drain dimensions at sites 1–10 from Watzlaf *et al.* (2000a), site 11 from Cravotta and Trahan (1999), site 12 from Cravotta and Weitzel (2002), and site 13 this report (C. A. Cravotta, unpublished data).

[b]Purity expressed as weight percent $CaCO_3$.

[c]Bulk volume computed as product of length·width·depth assuming tabular shape, except for Orchard. Orchard consisted of three parallel, semicircular troughs, each with a cross-sectional area of 0.244 m^2 and a length of 24.4 m (Cravotta and Trahan, 1999).

[d]Bulk density computed as initial limestone mass divided by bulk volume, $\rho_B = M_0/V_B$ [Eq. (3)]. Porosity and void ratio computed on basis of Eq. (4), $\phi = (\rho_S - \rho_B)/\rho_S$, assuming constant particle density, $\rho_S = 2650\,kg/m^3$ (Cravotta and Trahan, 1999).

Buck Mountain. Seepage from a collapsed drainage tunnel is collected at various points where water upwells along the length of the drain. Influent water quality is based on historical data and an adjacent seep. Access wells were installed at seven locations along the length of the drain. Perforated piping was installed along the length of the drain for flushing of accumulated solids.

Hegins. Discharge from a collapsed mine tunnel is piped into the drain, which consists of four cells in series. Influent is accessible before contacting limestone. Outflow spills from the top of each cell into the next. Access wells were installed at four locations in each of the cells. Perforated piping with valves for each cell was installed along the length of the drain for flushing of accumulated solids. At the time of this report, the Hegins drain had not been buried nor completely flooded.

The Orchard and Hegins drains were designed as OLDs for treatment of "oxic" influent that nonetheless contained relatively low concentrations of total Fe (<3 mg/liter). Drains at the other sites were previously classified as ALDs (Hedin and Watzlaf, 1994; Watzlaf *et al.*, 2000a). Data on dissolved O_2 and Fe^{3+} concentrations in *influent* to many of these drains were not available to confirm their ALD classification. However, previously reported data on the difference in concentration of Fe^{3+} between influent and effluent for the Howe Bridge 1, Howe Bridge 2, Morrison, Jennings, and REM-R drains (Hedin and Watzlaf, 1994) indicate that only the first three drains, which treated influent containing <1 mg/liter of Fe^{3+}, were unambiguously ALDs. The Jennings and REM-R drains treated influent that contained ≥10 mg/liter of Fe^{3+}, indicating that these should be classified as OLDs (>1 mg/liter of Fe^{3+}, Al^{3+}, or O_2). Hence, in this report, ALDs and OLDs are considered together to characterize limestone drain treatment systems generally, and then differences in treatment effectiveness are examined that could result from different factors, such as detention time and influent compositions, including pH and redox state.

B. Methods of Sampling and Analysis

Details of the field and laboratory methods for water-quality sampling and analysis were reported previously (Watzlaf and Hedin, 1993; Hedin and Watzlaf, 1994; Hedin *et al.*, 1994b; Cravotta and Trahan, 1999; Watzlaf *et al.*, 2000a). Standard methods were used for field analysis of pH, alkalinity (pH 4.5 end point), temperature, and specific conductance on unfiltered samples (e.g., Wood, 1976; Wilde *et al.*, 1998) and for laboratory analysis of acidity (pH 8.3 end point), major ions, and various metals (e.g., Greenberg

et al., 1992; Fishman and Friedman, 1989). Samples for analysis of dissolved metals were filtered through 0.45-μm pore-sized filters. Outflow from each of the drains was accessible for volumetric flow measurement and water-quality monitoring; however, only the Howe Bridge 1, Howe Bridge 2, Elklick, Morrison, Orchard, Buck Mountain, and Hegins drains had sampling access wells at intermediate points between inflow and outflow. Samples were retrieved from access wells by use of pumps or bailers. The actual inflow was not accessible at a majority of the drains, thus adjacent untreated seeps that had similar character as the untreated AMD were sampled or historical data for the untreated AMD were used to represent the influent. However, use of historical data to represent influent water quality may overestimate contaminant levels because water quality of untreated AMD commonly improves with time (e.g., Wood, 1996). Generally, flow rate and water quality at each drain were monitored quarterly or more frequently during the first year after the drains were constructed and less frequently during subsequent years.

The long-term averages for flow rate, pH, net acidity (acidity–alkalinity), alkalinity, and concentrations of solutes in influent and effluent of the 13 limestone drains were compiled or computed for subsequent evaluation of effects of limestone drain treatment on the neutralization of acidity and attenuation of metals transport (Table II). On the basis of water-quality data for many of the sites considered, as reported by Hedin and Watzlaf (1994) and Cravotta and Trahan (1999), activities of aqueous species, P_{CO_2}, and mineral saturation indices were calculated using the WATEQ4F computer program (Ball and Nordstrom, 1991). The saturation index (SI) provides a basis for evaluating the potential for dissolution or precipitation of a solid phase (Stumm and Morgan, 1996). Values of SI that are negative (< -0.1), approximately zero (± 0.1), or positive (> 0.1) indicate the water is undersaturated, saturated, or supersaturated, respectively, with the solid phase. If undersaturated, the water can dissolve the solid phase. If supersaturated, the water cannot dissolve the solid phase but can potentially precipitate it.

Additionally, to evaluate dissolution and precipitation effects at the Orchard drain, limestone samples that had been measured for weight, density, porosity, and geometric surface dimensions (thickness, width, length) were suspended with braided nylon chord and then retrieved and remeasured after 5 months to 5 years elapsed time of immersion. The retrieved samples were used to determine the rate of limestone dissolution at a particular location and the chemistry and mineralogy of encrustation. The dissolution rate was normalized with respect to the geometric surface area of the sample so that the field results could be compared with rate estimates from published laboratory experiments (Cravotta and Trahan, 1999).

Finally, empirical test results for the Howe Bridge 1 and Morrison sites that had previously been reported by Watzlaf and Hedin (1993) are used in

Table II

Average[a] Quality of Influent (In) and Effluent (Eff) at 13 Limestone Drains in Pennsylvania and Maryland

Limestone drain site[b]	pH (units)		Net acidity[c] (mg/liter as $CaCO_3$)		Alkalinity (mg/liter as $CaCO_3$)		Sulfate (mg/liter)		Calcium[d] (mg/liter)		Iron[e] (mg/liter)		Manganese (mg/liter)		Aluminum[e] (mg/liter)		Cobalt (mg/liter)		Nickel (mg/liter)		Zinc (mg/liter)	
	In	Eff	In	Eff	In	Eff	In	Eff	In	Eff	In	Eff	In	Eff	In	Eff	In	Eff	In	Eff	In	Eff
1. Howe Bridge 1	5.7	6.3	472	352	33	155	1300	1300	157	209	276	275	41	41	< 0.2	< 0.2	0.48	0.48	0.51	0.50	0.62	0.55
2. Howe Bridge 2	5.4	6.5	411	274	35	163	1200	1200	154	206	250	248	37	36	< 0.2	< .2	0.39	0.39	0.40	0.40	0.42	0.39
3. Elklick	6.1	6.7	52	−63	34	159	330	330	*77*	129	59	53	4.8	4.9	< 0.2	< .2	0.07	0.07	0.10	0.09	0.13	0.08
4. Jennings	3.2	6.2	280	−34	0	139	630	620	*83*	208	76	59	8.4	8.3	20.9	1.1	0.13	0.15	0.40	0.40	0.66	0.54
5. Morrison	5.2	6.4	387	51	29	278	1300	1000	115	223	*207*	156	49	41	0.5	< 0.2	0.86	0.75	0.79	0.65	0.95	0.72
6. Filson-R	5.7	6.5	100	−139	48	299	410	440	69	189	59	55	20	20	0.4	< 10.2	0.23	0.23	0.18	0.18	0.27	0.18
7. Filson-L	5.7	6.6	104	−175	48	317	410	400	69	180	59	55	20	16	0.4	< 10.2	0.23	0.13	0.18	0.10	0.27	0.17
8. Schnepp	3.3	6.2	225	−43	0	168	980	750	*90*	198	*92*	61	28	26	6.7	< 0.2	NA[f]	0.27	NA	0.33	NA	0.34
9. REM-R	4.3	5.5	NA	835	0	54	2800	2400	*210*	232	*589*	447	136	126	4.5	3.2	NA	1.49	NA	1.54	NA	2.46
10. REM-L	NA	6.0	NA	259	NA	113	NA	1300	*150*	201	NA	185	NA	51	NA	< .2	NA	0.60	NA	0.66	NA	0.76
11. Orchard	3.6	6.1	57	−43	0	64	190	170	24	50	1.7	0.2	2.6	1.6	0.9	0.2	0.08	0.04	0.12	0.08	0.11	0.15

(continues)

Table II (*continued*)

Limestone drain site[b]	pH (units)		Net acidity[c] (mg/liter as $CaCO_3$)		Alkalinity (mg/liter as $CaCO_3$)		Sulfate (mg/liter)		Calcium[d] (mg/liter)		Iron[e] (mg/liter)		Manganese (mg/liter)		Aluminum[e] (mg/liter)		Cobalt (mg/liter)		Nickel (mg/liter)		Zinc (mg/liter)	
	In	Eff	In	Eff	In	Eff	In	Eff	In	Eff	In	Eff	In	Eff	In	Eff	In	Eff	In	Eff	In	Eff
12. Buck Mountain	4.5	6.5	30	−85	1	86	48	48	3	38	8.5	9.6	.6	0.8	0.5	0.1	0.04	0.03	0.05	0.03	0.06	0.03
13. Hegins	3.8	4.4	40	30	0	1	230	230	10	17	0.3	0.2	1.5	1.7	4.1	3.4	0.08	NA	0.12	NA	0.12	NA

[a] Average for period of record, not adjusted for frequency or time of sample collection.
[b] Data for influent and effluent quality at sites 1–10 from Watzlaf *et al.* (2000a) and at sites 11–13 this report (C. A. Cravotta, unpublished data from USGS NWIS data base). Influent data for sites 5–7 based on quality of nearby seep and for sites 8–10 and 12 based on quality of untreated discharge prior to drain construction.
[c] Net acidity = acidity − alkalinity; negative values indicate net alkaline conditions.
[d] Values in italics for influent calcium estimated on the basis of net alkalinity or net acidity.
[e] Values in italics for influent iron or aluminum indicate influent chemistry (Fe^{3+} or Al^{3+} > 1 mg/liter) that is inconsistent with design criteria for ALD (Hedin *et al.*, 1994a,b; Skousen *et al.*, 1998).
[f] Not available.

this chapter to indicate qualitative and quantitative effects of variable influent compositions, detention times, and limestone purity on limestone drain performance. Collapsible, 3.8-liter polyethylene containers, hereafter called "cubitainers," were loaded with 4 kg of 1.3- by-3.5-cm limestone fragments (two-thirds total volume), filled with the untreated mine water to exclude any air, and then maintained at field water temperature to evaluate the generation of alkalinity (Fig. 1). The untreated mine water at the sites initially contained some alkalinity but was net acidic: Howe Bridge (pH 5.7; $P_{CO_2} = 10^{-1.24}$; alkalinity = 39 mg/liter as $CaCO_3$; acidity = 516 mg/liter as $CaCO_3$) and Morrison (pH 5.4; $P_{CO_2} = 10^{-1.05}$; alkalinity = 29 mg/liter as $CaCO_3$; acidity = 460 mg/liter as $CaCO_3$). The cubitainer tests were conducted in duplicate using several local varieties of limestone with reported purity ranging from 82 to 99% by weight $CaCO_3$. The impurities consisted of $MgCO_3$, as well as noncarbonate components, such as silica, clay, and organic matter. Periodically over 11 days, samples were withdrawn through a valve to fill a 60-ml

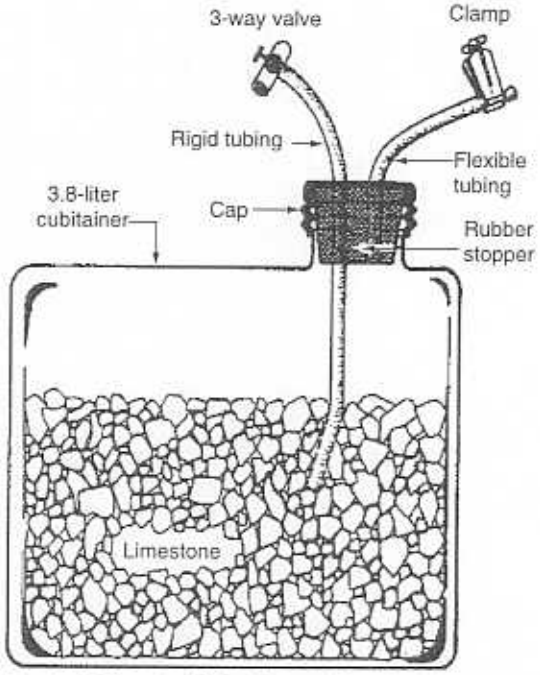

Figure 1 Schematic of a 3.8-liter "cubitainer" containing 4 kg limestone and filled with mine discharge water to evaluate alkalinity production rates (after Watzlaf and Hedin, 1993). Limestone sized to 1.3 × 3.5 cm. Cubitainer and tubing are impermeable to gas.

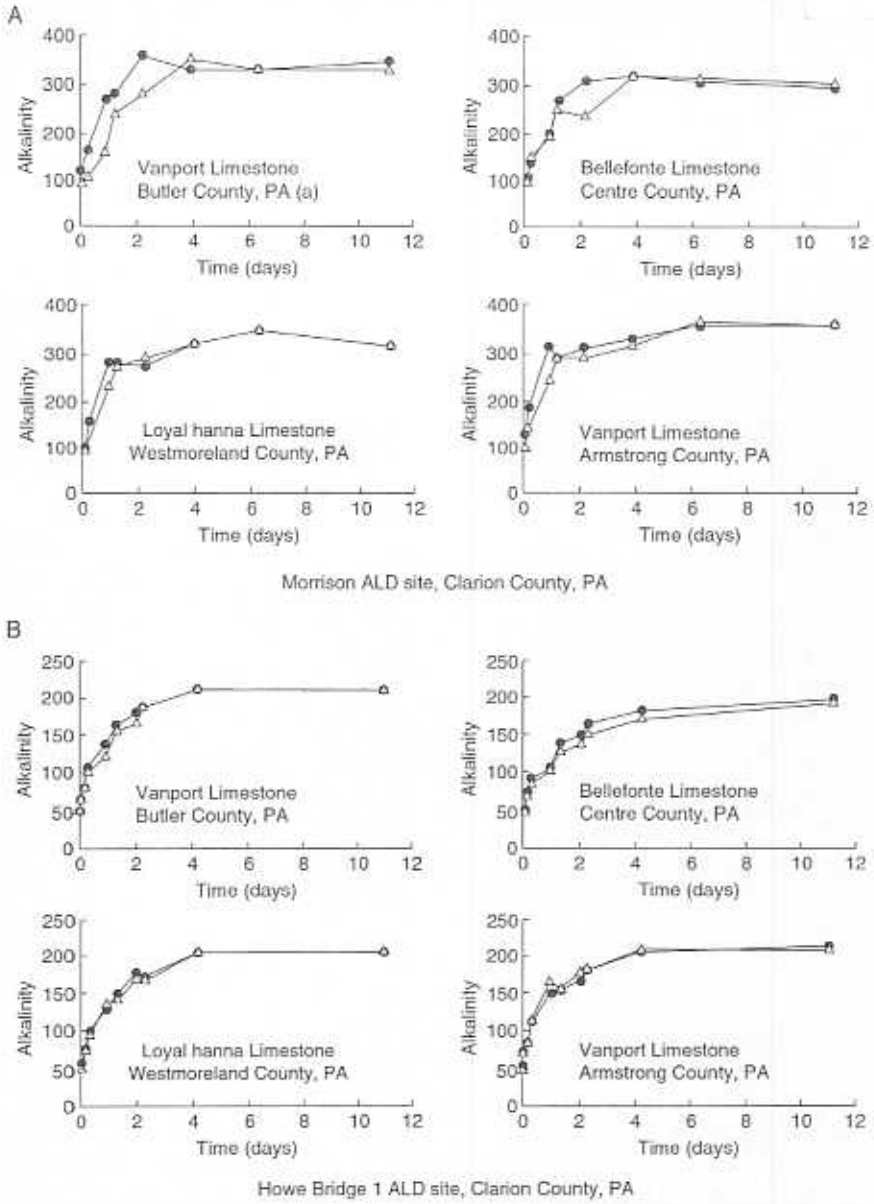

Figure 2 Alkalinity concentration (mg/liter as $CaCO_3$) generated during immersion of four limestone types from various locations by mine drainage from Morrison and Howe Bridge sites (after Watzlaf and Hedin, 1993). Each graph plots the alkalinity concentration in duplicate cubitainers (Δ, ○).

syringe after purging approximately 10 ml of fluid from the sample tubing. Each sample was forced through a 0.45-μm pore-sized filter and then analyzed for alkalinity (pH 4.5 end point) (Watzlaf and Hedin, 1993). Alkalinity data for the cubitainer tests were reported as time-series plots, some of which are shown in Fig. 2.

III. PERFORMANCE AND DESIGN OF LIMESTONE DRAINS

According to laboratory and field studies, such as those by Watzlaf and Hedin (1993), Hedin and Watzlaf (1994), and Cravotta and Trahan (1999), the concentration of alkalinity that is produced in a limestone bed and its effectiveness for increasing pH and removing dissolved metals from contaminated mine drainage depend on the composition of the water; the quantity, purity, and particle size of limestone; and the detention time and rates of chemical reactions. Typically, the pH and concentrations of alkalinity and Ca^{2+} increased asymptotically with increased detention time, or downflow distance, within a limestone bed (Figs. 2, 3A, 4, and 5). These trends generally result from a decrease in the rate of limestone dissolution as calcite equilibrium is approached (Figs. 5 and 6). With increased pH, concentrations of acidity and various dissolved metals may decrease due to precipitation and adsorption reactions within the limestone bed (Figs. 5 and 6). However, the occurrence and efficiency of these processes vary among different treatment systems.

Downgradient trends for pH, alkalinity, acidity, Ca, and other solute concentrations within the Orchard OLDs provide a useful basis for interpreting important chemical variations within limestone drains, generally. Downgradient trends for the first 6 months of treatment (Figs. 5A and 5B) are consistent with those expected for an ALD, except that Fe^{2+} transport generally would be conservative in an ALD (indicated by dashed line in Fig. 5B). In contrast, the downgradient trends after the first 6 months, when the drains began to retain Mn and trace metals (Fig. 5D), are consistent with those expected for OLDs (e.g., Cravotta and Trahan, 1999).

Hedin and Watzlaf (1994), Robbins *et al.* (1999), and Cravotta and Trahan (1999) showed that limestone theoretically could dissolve throughout the limestone drains they investigated because the water was consistently undersaturated with respect to calcite, attaining calcite saturation index ($SI_{CALCITE}$) values from −2.4 to −0.3 under the conditions evaluated. For example, despite increased pH, alkalinity, and Ca through the Orchard OLDs, the $SI_{CALCITE}$ remained negative (Fig. 6A). Solute concentrations, pH, and

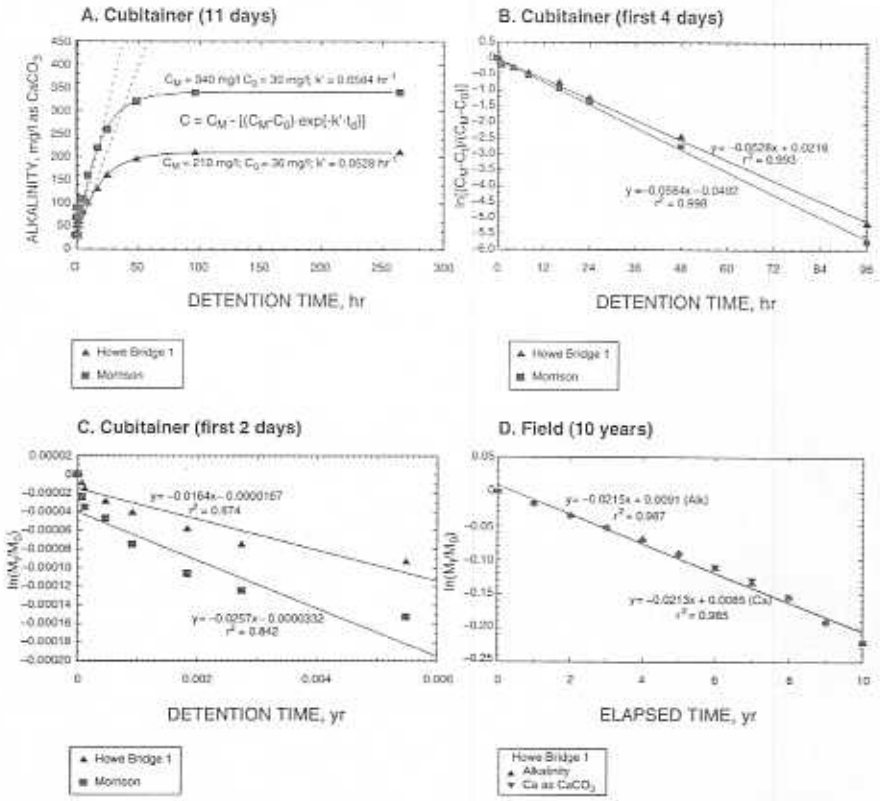

Figure 3 Dissolution rate data for 11-day cubitainer experiments and a 10-year field study. (A) Generalized alkalinity data points for cubitainer tests from Fig. 2. (B) Natural logarithm of the difference between steady-state maximum alkalinity (C_M) and measured alkalinity (C_T) divided by the difference between C_M and initial alkalinity (C_0) versus time. Slope indicates rate constant, k', for computation of alkalinity. (C and D) Natural logarithm of remaining limestone mass (M_t) divided by initial mass (M_0) versus time. Slope indicates rate constant, k, for computation of limestone mass. Field data for the Howe Bridge limestone drain are based on reported initial limestone mass and limestone purity (Table I) and annual averages for flow rate and concentrations of alkalinity and Ca in effluent and influent.

$SI_{CALCITE}$ increased most rapidly near the inflow (Figs. 5 and 6A). Cravotta and Trahan (1999) explained that for a computed detention time of 1 h, the water in the Orchard OLDs was net alkaline and had pH ~ 6 and $SI_{CALCITE} -2$; however, by tripling the detention time from 1 to 3 h, pH increased only to ~ 6.8, whereas $SI_{CALCITE}$ increased to -1 and alkalinity and Ca concentrations doubled from about 60 to 120 and 90 to 180 mg/liter, respectively. These observations are consistent with the asymptotic trends for

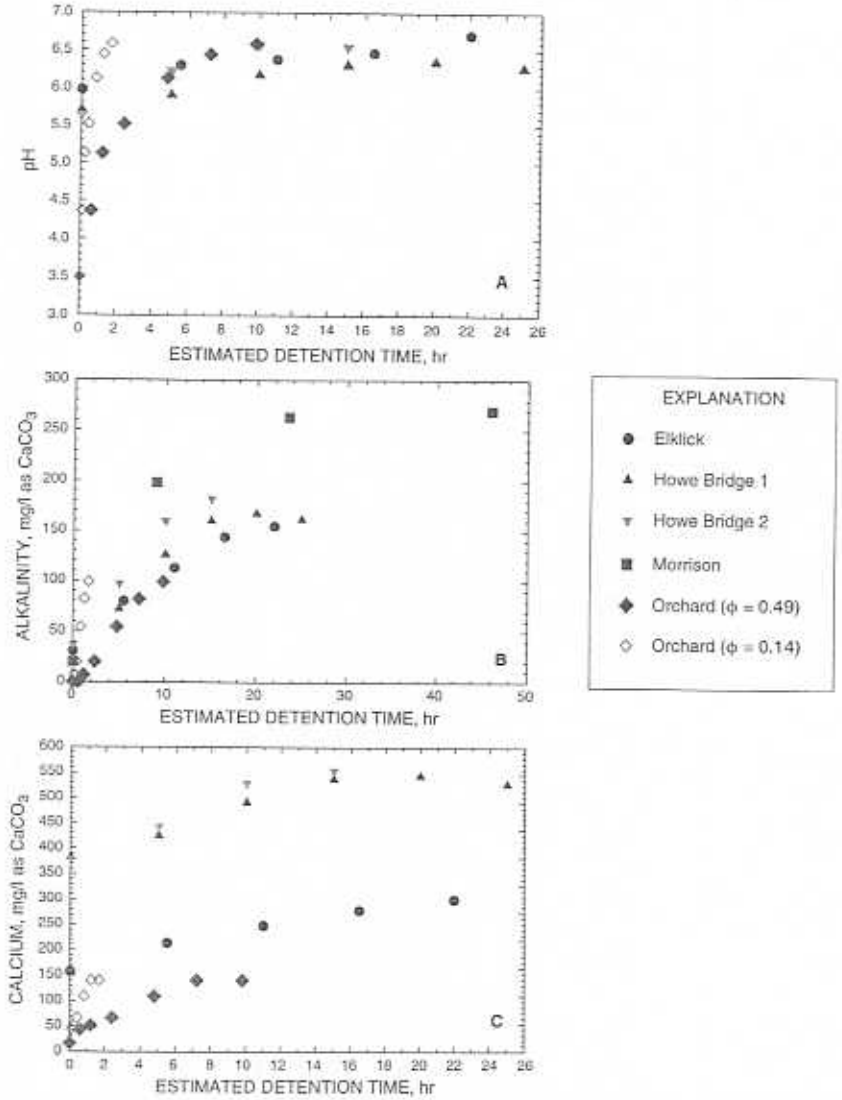

Figure 4 Changes in pH, alkalinity, and Ca concentration with detention time (downflow distance) of contaminated mine drainage within limestone drains at Elklick, Howe Bridge 1 and 2, Morrison, and Orchard sites described in Table I. Detention time computed as a product of porosity (ϕ), downflow distance (L), and cross-sectional area (A) divided by flow rate (Q): $t_d = \phi \cdot L \cdot A/Q$, assuming $\phi = 0.49$ (solid symbols). Data for Orchard also are displayed for $\phi = 0.14$ (open symbols) computed for initial limestone mass and drain volume (Table I).

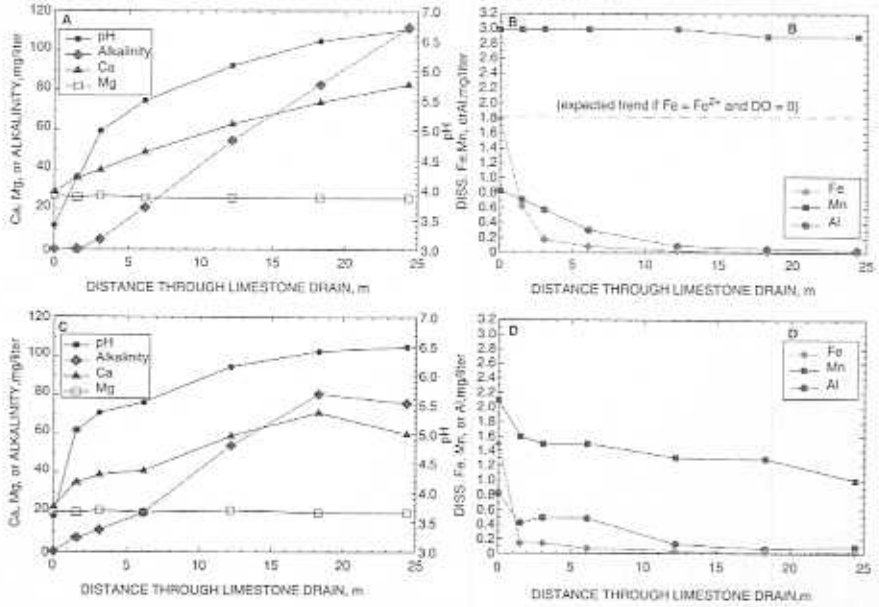

Figure 5 Sequential changes in water chemistry within Orchard limestone drain. Averages for March–August, 1995: (A) pH and concentrations of alkalinity, Ca, and Mg and (B) concentrations of dissolved Fe, Mn, and Al. Averages for September 1995–May 2000: (C) pH and concentrations of alkalinity, Ca, and Mg (D) concentrations of dissolved Fe, Mn, and Al.

a decreased alkalinity production rate with an increased detention time for cubitainer and field tests at other sites (Figs. 2 and 4). Hence, the detention time is a critical variable determining the performance of limestone drains. Furthermore, although the asymptotic trends for alkalinity production with detention time (Figs. 2 and 4) could be interpreted to indicate decreasing rates of limestone dissolution as equilibrium with calcite is approached, they could also indicate decreased limestone dissolution and/or alkalinity production rates because of the accumulation of secondary minerals.

The precipitation of secondary minerals may result in limestone drains due to increases in pH, alkalinity, and Ca concentrations. For example, gypsum ($CaSO_4 \cdot 2H_2O$) and hydrous oxides of Fe(III) and Al could precipitate within limestone beds if concentrations of SO_4^{2-}, Fe^{3+}, and Al^{3+} in influent are elevated (Figs. 6B, 6C, and 6D). Hedin and Watzlaf (1994) and Robbins *et al.* (1999) showed that except where concentrations of SO_4 exceeded about 2000 mg/liter, the water within limestone drains remained undersaturated with respect to gypsum. As the concentration of Ca increased within the Orchard OLD, gypsum saturation index (SI_{GYPSUM}) values increased but

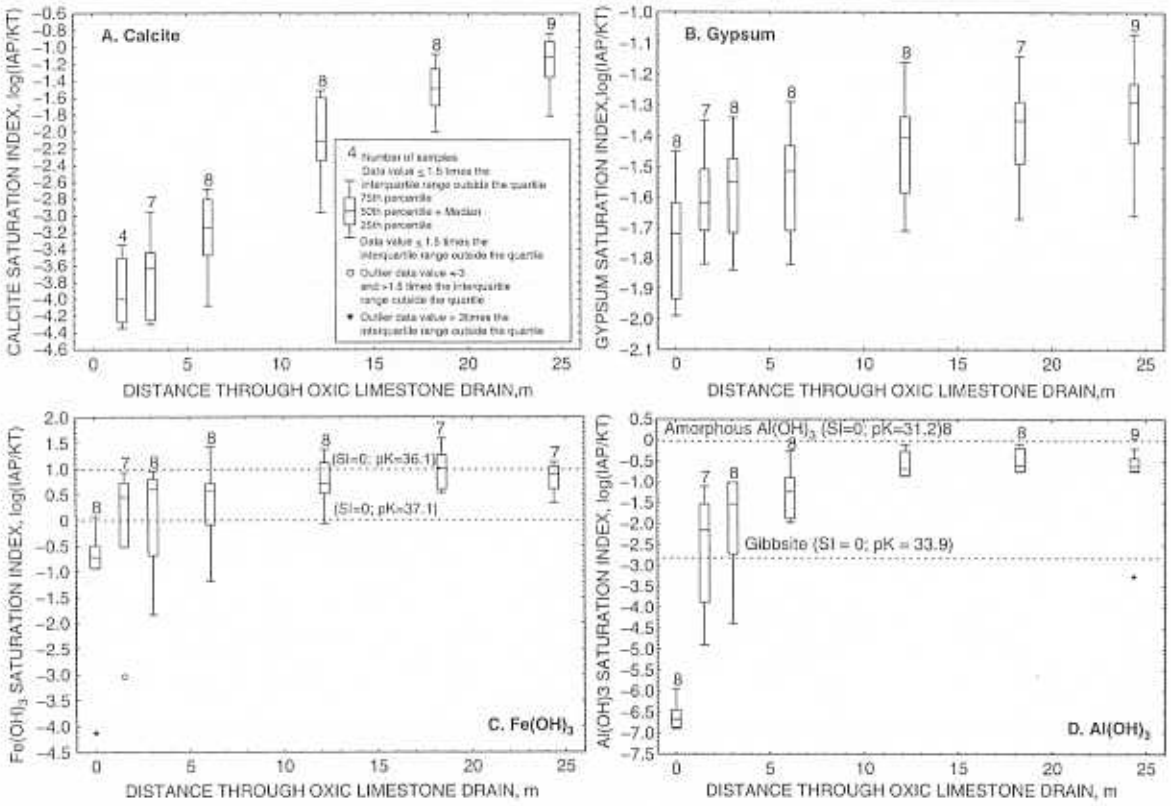

Figure 6 Sequential changes in saturation with respect to various minerals that could dissolve or precipitate within Orchard limestone drain (after Cravotta and Trahan, 1999). Saturation index calculated using the WATEQ4F computer program (Ball and Nordstrom, 1991). Data for samples collected March 1995–March 1996. From Cravotta and Trahan (1999).

remained well below equilibrium (Fig. 6B), hence precipitation of this mineral on limestone surfaces was unlikely. Nevertheless, even at sites where the SI_{GYPSUM} was positive, indicating a potential for gypsum precipitation, SO_4^{2-} transport generally was conservative (Hedin and Watzlaf, 1994), indicating that the precipitation of gypsum was not an effective attenuation mechanism for this constituent. In contrast, the precipitation of Al^{3+} and Fe^{3+} is likely within limestone drains because of the low solubilities of these metals (e.g., Stumm and Morgan, 1996). The precipitation of hydrous oxides of Al and Fe(III) accounted for quantitative removal of the dissolved Al and Fe within the Orchard OLDs. Although dissolution features were visible, calcite and limestone samples immersed in the drain were coated, at least locally, by these secondary minerals (Robbins *et al.*, 1999). The formation and accumulation of any of these minerals within a limestone bed could pose a problem if they were to armor the limestone surfaces or clog pore spaces, impeding flow through the bed.

A. Porosity and Detention Time

Detention time (t_d) and, hence, rates of alkalinity production or other effects of limestone dissolution within limestone beds can be estimated on the basis of volumetric flow rate (Q) and estimated void volume (V_V) within the bed,

$$t_d = V_V/Q \tag{1}$$

or

$$t_d = \phi \cdot V_B/Q \tag{2}$$

where V_B is the bulk volume and ϕ is the porosity ($\phi = V_V/V_B$). If the total mass of limestone (M) and bulk volume (V_B) of the drain are known, porosity can be computed. According to Freeze and Cherry (1979), bulk density (ρ_B) is defined as

$$\rho_B = M/V_B \tag{3}$$

and is proportionally related to porosity (ϕ) by the stone density (ρ_S) where

$$\rho_B = \rho_S \cdot (1 - \phi). \tag{4}$$

Hence, by rearranging Eq. (4) and assuming $\rho_S = 2.65\,g/cm^3$ considered typical for limestone (Freeze and Cherry, 1979; Cravotta and Trahan, 1999), porosity can be determined for various bulk densities and vice versa:

$$\phi = 1 - (\rho_B/\rho_S). \tag{5}$$

Knowing ρ_S, ϕ, and Q, Eq. (2) can be rewritten by substituting $V_B = M/[\rho_S \cdot (1 - \phi)]$ in accordance with Eqs. (3) and (5) to determine the detention time for water flowing through a limestone drain with a given mass

$$t_d = M/[Q \cdot \rho_S \cdot (1 - \phi)/\phi] \tag{6}$$

or the mass of limestone required to achieve a given detention time

$$M = t_d \cdot [Q \cdot \rho_S \cdot (1 - \phi)/\phi]. \tag{7}$$

For the 13 limestone drains evaluated in this chapter, computed porosities ranged from 0.12 to 0.50, with a median of 0.34; the median bulk density was 1756 kg/m^3 (Table I). The corresponding detention times for the given porosities and average flow at these sites ranged from 1.3 to 33 h (Table III). Many of the computed porosity values are less than a reference value of 0.49 based on precise, laboratory measurements; laboratory porosity ranged from 0.38 to 0.50 for well-sorted limestone fragments, with higher values associated with larger (5.1 to 7.6 cm) particles (Rice *et al.*, 1970; Hedin and Watzlaf, 1994). Lower porosities, e.g., 0.14 for the Orchard limestone drain (Table I), were explained by Cravotta and Trahan (1999) as possibly resulting from compaction of mixed-size, tabular limestone fragments; rough or flexible outside walls; and/or the accumulation of secondary minerals. Nevertheless, the computed porosity of 0.12 for the Howe Bridge 2 limestone drain probably is lower than its actual porosity. The authors suspect that reported dimensions for this drain are inaccurate; however, construction data could not be verified. Furthermore, although mass estimates are based on the delivered weight of limestone, accidental spillage and intentional spreading outside the drain could be significant. Some reported weights account for this wastage, whereas others do not. Tracer tests reported by Watzlaf *et al.* (2000a) and Cravotta and Trahan (1999), which directly indicate detention time(s), were interpreted to be consistent with the previously reported porosities at these drains. However, tracer tests and longitudinal sampling at the respective study sites indicated complex, preferential flow paths caused by a range of porosities and other hydrological controls. Hence, different estimates of detention time are possible considering the uncertainty and range of porosities.

Table III and Fig. 4 show that porosity is a critical variable for characterizing a limestone drain. For example, estimated detention times using the computed porosity of 0.36 for the drain at the Howe Bridge 1 site are approximately one-half of those computed using an assumed porosity of 0.49, and detention times for Orchard drain vary by almost a factor of 6 considering the computed porosity of 0.14 and reference value of 0.49. Furthermore, the same mass of limestone would occupy a two-thirds larger volume for $\phi = 0.49$ than for $\phi = 0.14$. Hence, consistent and accurate

Table III

Limestone Dissolution Rate and Associated Changes in Limestone Mass and Detention Time for 13 Limestone Drains in Pennsylvania and Maryland

Limestone drain site[a]	Year built[a] ($t = 0$)	Current age, $t = 2001$ (years)	Mass limestone[a,b]		Average flow rate,[a] Q (liters/min)	Average Ca concentration[a,c]			Average flux of Ca as $CaCO_3$,[c] J_{CaCO_3} (tonne/year)	Limestone dissolution rate,[d] k ($year^{-1}$)	Detention time[e]			
			Initial, M_0 (tonne)	Current, M_{2001} (tonne)		Influent (mg/liter)	Effluent (mg/liter)	Net as $CaCO_3$ (mg/liter)			Initial, t_{i0} (h)		Current, t_{i2001} (h)	
											$\phi =$ est.	$\phi =$ 0.49	$\phi =$ est.	$\phi =$ 0.49
1. Howe Bridge 1	1991	10	455.0	314.8	96.8	157	209	130.0	6.62	0.018	16.6	28.4	13.9	23.8
2. Howe Bridge 2	1993	8	132.0	103.4	48.4	154	206	130.0	3.31	0.031	2.4	16.5	1.9	12.9
3. Elklick	1994	7	165.0	147.2	37.1	77	129	130.0	2.54	0.018	17.9	26.9	15.8	23.7
4. Jennings	1993	8	365.0	308.9	73.4	83	208	312.1	12.06	0.037	20.5	30.0	15.3	22.4
5. Morrison[c]	1990	11	65.0	51.0	8.0	115	223	270.0	1.14	0.019	26.0	49.1	21.1	39.8
6. Filson-R[c]	1994	7	590.0	541.1	44.0	69	189	299.5	6.93	0.013	29.8	81.0	27.2	73.8
7. Filson-L[c]	1994	7	635.0	618.3	31.2	69	180	277.0	4.55	0.008	33.0	123	31.2	116
8. Schnepp	1993	8	130.0	105.0	19.8	*90*	198	270.0	2.81	0.024	15.1	39.7	12.4	32.7
9. REM-R	1992	9	125.0	89.3	112.0	*210*	232	55.0	3.24	0.032	7.1	6.7	5.4	5.1
10. REM-L	1992	9	125.0	73.3	96.2	*150*	201	127.5	6.45	0.063	7.9	7.9	4.5	4.5
11. Orchard	1995	6	38.1	32.3	30.0	24	50	64.3	1.01	0.027	1.3	7.7	1.1	6.5

(*continues*)

Table III (*continued*)

Limestone drain site[a]	Year built[a] ($t = 0$)	Current age, $t = 2001$ (years)	Mass limestone[a,b] Initial, M_0 (tonne)	Mass limestone[a,b] Current, M_{2001} (tonne)	Average flow rate,[a] Q (liters/min)	Average Ca concentration[a,c] Influent (mg/liter)	Average Ca concentration[a,c] Effluent (mg/liter)	Average Ca concentration[a,c] Net as $CaCO_3$ (mg/liter)	Average flux of Ca as $CaCO_3$,[c] J_{CaCO_3} (tonne/year)	Limestone dissolution rate,[d] k ($year^{-1}$)	Detention time[e] Initial, t_{d0} (h) ϕ = est.	Detention time[e] Initial, t_{d0} (h) ϕ = 0.49	Detention time[e] Current, t_{d2001} (h) ϕ = est.	Detention time[e] Current, t_{d2001} (h) ϕ = 0.49
12. Buck Mountain	1997	4	320.0	233.5	504.0	3	38	87.5	23.19	0.079	1.8	3.8	1.3	2.8
13. Hegins	2000	1	800.0	789.7	1000.0	10	17	17.8	9.34	0.013	2.9	4.8	2.8	4.8
Median		8	165.0		48.4			130.0	4.55	0.024	15.1	26.9	12.4	22.4

[a] Influent concentrations for sites 5–7 based on water quality of nearby seep and for sites 8–10 and 12 based on water quality of untreated discharge prior to drain construction. Average for monitoring period not adjusted for frequence or time of sample collection. Values in italics for influent Ca estimated on basis of net alkalinity or net acidity (Table III) for computations of $CaCO_3$ mass flux and limestone dissolution rate.

[b] Current mass of limestone computed on basis of Eq. (14), $M_{2001} = M_0 \cdot \exp\{-k \cdot t\}$, where t is current age and k is limestone dissolution rate.

[c] Net concentration of Ca as $CaCO_3$(ΔCa_{CaCO_3}) computed as difference between concentration in effluent and influent, multiplied by 2.5. Average flux of Ca as $CaCO_3$ computed as the product of average flow rate and net Ca concentration, $J_{CaCO_3} = Q \cdot \Delta Ca_{CaCO_3}$ [Eq. (11)].

[d] Limestone dissolution rate, $k = J_{CaCO_3}/(M_0 \cdot X_{CaCO_3})$, computed on the basis of Eq. (12) as average flux of Ca as $CaCO_3$ divided by the product of initial mass of limestone and limestone purity (Table I).

[e] Detention time computed on basis of Eq. (6), $t_d = M_t/[Q \cdot \rho_S \cdot (1 - \phi)/\phi)]$, for average flow rate, using porosity estimates in Table I or assuming porosity of 0.49, and assuming constant particle density, $\rho_S = 2650\,kg/m^3$ (Cravotta and Trahan, 1999). Initial and current detention time computed for initial mass (M_0) and current mass (M_{2001}) of limestone, respectively.

estimates of porosity, bulk volume, and mass of limestone are needed to determine the necessary space required for construction and to obtain the desired detention time for effluent through a limestone drain.

B. Alkalinity Production Rate

Effluent from each of the 13 drains had higher pH, alkalinity, and Ca concentrations and lower acidity than the influent (Table II) because of limestone dissolution within the drains. The extent of change in these parameters varied among the drains due to differences in influent chemistry, detention time, and limestone dissolution rate (Table III). Although concentrations of alkalinity and Ca in effluent were not correlated with detention time among the different drains (Table II), changes in pH and other chemical variables generally were expected to be greatest near the inflow and diminished with increased detention time or distance from the inflow in each of the drains. For example, longitudinal monitoring data for Elklick, Howe Bridge 1 and 2, Morrison, and Orchard limestone drains (Fig. 4) and cubitainer test data for the Howe Bridge 1 and Morrison drains (Figs. 2 and 3A) all indicated that the rate of alkalinity production decreased with increased detention time. The cubitainer tests indicated, for the same influent, that the generation of alkalinity within the containers did not vary with limestone purity. Furthermore, the cubitainer tests showed that alkalinity approached a steady-state, maximum concentration after about 48 h that was equivalent to that for effluent from the respective limestone drains (Figs. 2 and 4). The maximum alkalinity for the Morrison cubitainer tests was approximately 350 mg/liter, whereas that for the Howe Bridge tests was approximately 210 mg/liter (Fig. 3A). Watzlaf and Hedin (1993) attributed differences in alkalinity production between the Morrison and the Howe Bridge tests to differences in influent Pco_2 and pH.

According to Lasaga (1981), the first-order kinetics relation for a steady-state condition as observed for the cubitainer tests can be written as

$$dC/dt = k' \cdot (C_M - C), \tag{8}$$

where C is the alkalinity (or Ca) concentration as $CaCO_3$, C_M is the steady-state or maximum concentration, and k' is the rate constant that has units of inverse time (1/time). Integration of Eq. (8) yields:

$$\ln[(C_M - C_t)/(C_M - C_0)] = -k' \cdot t_d, \tag{9}$$

where C_0 is the initial concentration and C_t is the concentration at any detention time. A logarithmic plot of $[(C_M - C)/(C_M - C_0)]$ versus detention time will yield a straight line with slope of $-k'$ for a first-order reaction

(Lasaga, 1981). Figure 3B shows these plots on the basis of generalized time-series data for the Howe Bridge 1 and Morrison cubitainer tests. The linear slopes indicate values for k' of 0.053 and 0.058 h^{-1} for Howe Bridge 1 and Morrison, respectively.

Taking the logarithm and rearranging Eq. (9), alkalinity concentration at any detention time can be computed as a function of these rate constants *and* the initial and maximum alkalinities:

$$C_t = C_M - [(C_M - C_0) \cdot \exp\{-k' \cdot t_d\}]. \quad (10)$$

The solid curves drawn through the generalized cubitainer data points in Fig. 3A were computed on the basis of Eq. (10) and the corresponding generalized data from the cubitainer tests for the Howe Bridge 1 and Morrison limestone drains.

C. Limestone Dissolution Rate

For a limestone-based treatment system, the mass of limestone dissolved over time can be determined by measuring the $CaCO_3$ mass flux (J_{CaCO_3})

$$J_{CaCO_3} = Q \cdot \Delta C_{CaCO_3}, \quad (11)$$

where Q is the average flow rate and ΔC_{CaCO_3} is the difference between effluent and influent concentrations of acidity, alkalinity, or Ca expressed as $CaCO_3$. Generally, data for Ca concentrations are preferred over alkalinity or net acidity for computation of the $CaCO_3$ flux. Alkalinity cannot be measured at pH < 4.5, and acidity data generally are less precise and less accurate than those for Ca. For most sites, only the long-term averages for flow rate and ΔC_{CaCO_3} were available (Tables II and III). Hence, the limestone dissolution rate or decay constant, k, with units of inverse time at each of the drains was estimated as the long-term average Ca ion flux rate, J_{CaCO_3}, normalized by the initial mass and weight fraction $CaCO_3$ (X_{CaCO_3}) of the limestone:

$$k = J_{CaCO_3}/(M_0 \cdot X_{CaCO_3}). \quad (12)$$

For the 13 drains, estimates of k computed using Eq. (12) ranged from 0.008 to 0.079 $years^{-1}$ (Table III). Figure 7 illustrates differences in the projected remaining mass of limestone for this range of k values and assuming linear or exponential decay of the same initial mass. Large differences among the decay trends with increasing time for different decay constants indicate the importance of this parameter.

For a decreasing quantity over time, a first-order decay equation can be written as

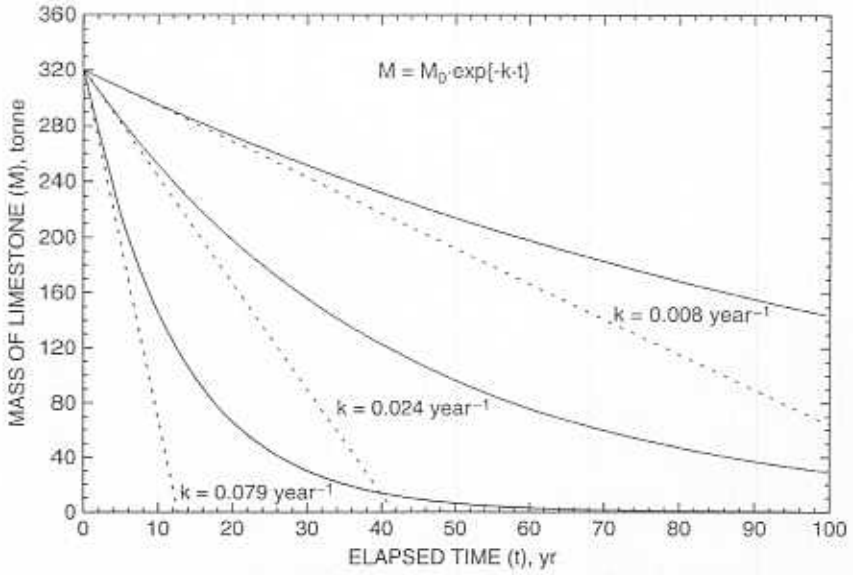

Figure 7 Change in mass of limestone with age of limestone drain considering initial mass of 320 tonne, various rate constants (k), and exponential decay (solid lines) or constant mass flux (dashed lines; x intercept is the inverse of the rate constant).

$$-dM/dt = k \cdot M, \tag{13}$$

where the quantity M typically has units of mass or concentration and k is the rate constant (Lasaga, 1981). Equation (13) applies to a variety of important geochemical processes, including radioactive decay, the oxidation of ferrous iron, and, as demonstrated in this chapter, the dissolution of limestone in an ALD or OLD. Integration of Eq. (13) yields the exponential decay expression

$$M_t = M_0 \cdot \exp\{-k \cdot t\}, \tag{14}$$

where M_0 is the initial quantity and M_t is the remaining quantity after continuous dissolution over elapsed time, t.

Although the assumption of constant (linear) $CaCO_3$ flux is reasonable for a relatively large mass of limestone, a small flux of $CaCO_3$, and a short initial time period, the linear and exponential decay trends diverge as time increases (Fig. 7). Because of this divergence, values of k derived using the time-averaged $CaCO_3$ flux [Eq. (12)] could decrease with elapsed time. For example, at the Orchard OLD, the average $CaCO_3$ flux decreased from 1.6 tonne/year for the first year of operation (Cravotta and Trahan, 1999) to 1.0 tonne/year for the 5-year average (Table III). The corresponding

dissolution rate constant decreased from an initial estimate of 0.042 $year^{-1}$ (Cravotta and Trahan, 1999) to 0.027 $year^{-1}$ for the 5-year average (Table III). Decreases in alkalinity concentration and corresponding decreases in the $CaCO_3$ flux and estimated limestone dissolution rates with age were also observed for the Howe Bridge 1 ALD. At this site, the average $CaCO_3$ flux for the first 3 years was 6.5 tonne/year (Hedin and Watzlaf, 1994) and that for the 10-year average was 6.1 tonne/year (Table III). The decreased $CaCO_3$ flux is expected as the remaining mass of limestone decreases through time.

The limestone dissolution rate, or exponential decay constant, can be determined by taking the logarithm of Eq. (14) and rearranging to

$$\ln (M_t/M_0) = -k \cdot t. \tag{15}$$

For a first-order process or reaction, a logarithmic plot of M_t/M_0 versus time will yield a straight line with slope $= -k$. For example, plots of $\ln(M_t/M_0)$ versus time were generated using annual averages for 10 years of monitoring at the Howe Bridge 1 drain (Fig. 3D). For each year, estimates of J_{CaCO_3} were computed using data for Ca and alkalinity concentrations [Eq. (11)] and were then divided by the reported limestone purity to estimate the incremental dissolved mass of limestone and hence the remaining mass. The resultant slopes from the plots of $\ln(M_t/M_0)$ versus time indicated k of 0.021 $year^{-1}$. This value is in good agreement with an estimate of 0.018 $year^{-1}$ derived using the long-term average Ca ion flux for Howe Bridge 1 (Table III).

Data for cubitainer experiments were also used to estimate limestone dissolution rate constants for the Howe Bridge 1 and Morrison limestone drains (Fig. 3C). An initial limestone mass of 4.0 kg and an initial solution volume of 2.3 liter were assumed. The initial solution volume was computed as the difference between the initial 3.8-liter total volume and the 1.5-liter limestone volume ($V_S = M_S/\rho_S = 4.0\,kg/2.65\,kg/liter$). Due to the periodic removal of solution, the solution volume was reduced incrementally by 60 ml at each time step when alkalinity was determined. The remaining mass of limestone at each time step was determined by the difference between initial mass and the cumulative $CaCO_3$ mass added to the solution, which was computed as the product of overall change in alkalinity concentration ($\Delta C_{CaCO_3} = C_t - C_0$) and the remaining volume of solution (V_L), corrected for limestone purity:

$$M_t = M_0 - (\Delta C_{CaCO_3} \cdot V_L/X_{CaCO_3}). \tag{16}$$

Because detention times under field conditions were less than 50 h (Table III), data for only the first 2 days of cubitainer tests were used for the logarithmic plot of M_t/M_0 versus time, in years. The resultant slopes of the regression lines indicate that values for k would be 0.016 and 0.026 $year^{-1}$ for the Howe Bridge 1 and Morrison limestone drains, respectively (Fig. 3C). Considering

that k values ranged by a factor of 10 among the 13 drains evaluated, these estimates are in good agreement with values of 0.018 and 0.019 $year^{-1}$ derived on the basis of a 10-year average Ca ion flux for the respective limestone drains (Table III).

For the Orchard drain, limestone slabs immersed for 1 to 5 years near the middle of the drain dissolved at rates of 0.044 to 0.057 $year^{-1}$ (Table IV). These rates were comparable to the average k value of 0.027 $year^{-1}$ derived on the basis of long-term average Ca ion flux for the first 5 years of operation (Table III). Nevertheless, because of variations in chemistry along the length of the drain, the directly measured limestone dissolution rates varied by more than a factor of 5 between inflow and midflow points, with greatest rates near the inflow where the pH was least (Table IV). Hence, direct estimates of the limestone dissolution rate must consider the location of the limestone along the flow path through the drain and the possibility for variations in water chemistry at the location. In contrast, the dissolution rate estimated using average Ca or alkalinity flux integrates along the length of the drain and through time, making this estimate more useful as a measure of overall drain performance.

The rate of limestone dissolution within a bed is expected to vary as the chemical composition of the water changes and/or the flow rate changes, affecting detention time and chemistry along the flow path. Directly measured $CaCO_3$ dissolution rates within the Orchard OLD were greatest near the inflow, where $SI_{CALCITE}$ was minimal, and decreased with increased pH and activities of Ca^{2+} and HCO_3^- and decreased Pco_2 at downflow points (Table IV, Fig. 6A). These trends as a function of solution composition are consistent with rate laws established by laboratory experiments (Plummer *et al.*, 1979; Morse, 1983; Arakaki and Mucci, 1995). During the first 5 months, the limestone dissolution rate was 0.439 $year^{-1}$ at the inflow and 0.081 $year^{-1}$ at the midflow. However, lower dissolution rates of 0.044 to 0.057 $year^{-1}$ were determined for samples immersed at the midflow for periods of 1 to 5 years (Table IV). This decline in the dissolution rate, directly determined by reduction in mass over elapsed time of immersion, is consistent with the decline in the estimated value of k computed using 1- and 5-year averages for $CaCO_3$ flux.

At the Orchard OLD, the field rates of limestone dissolution were intermediate to those for the other limestone drains evaluated (Table III). However, the field rates for limestone reaction with AMD were about an order of magnitude less than reported laboratory rates of calcite dissolution at comparable pH in hydrochloric acid (HCl) solutions (e.g., Plummer *et al.*, 1979; Morse, 1983; Arakaki and Mucci, 1995). Aschenbach (1995) demonstrated that calcite dissolved more rapidly in HCl solutions than in synthetic AMD (sulfuric acid solutions) for a given pH and that calcite remained indefinitely

Table IV

Dissolution Rate for Limestone Samples Immersed in Limestone Drain at Orchard Drift, Pennsylvania

Elapsed time of immersion[a]	Longitudinal distance downflow, L (m)[b]	Limestone dissolution rate: k (g/g/year)	Limestone dissolution rate: Log (mmol/cm^2/s)[c]	Mass of Fe–Al–Mn encrustation (mg)	Average hydrochemical values for time interval: pH	Partial pressure CO_2, log (atm)	Alkalinity (mg/liter as $CaCO_3$)	Net Ca concentration[d] (mg/liter as $CaCO_3$)
5 months	0	0.439	−6.86	800	3.4	> −0.6	0	0
	6.1	0.130	−7.39	415	5.5	−1.2	21	43
	12.2	0.081	−7.60	79	6.1	−1.4	51	78
12 months	0	NA[e]	NA	361[f]	3.4	> −0.6	0	0
	6.1	0.061	−7.74	108[f]	5.5	−1.2	21	47
	12.2	0.044	−7.89	126[f]	6.1	−1.4	54	86
60 months	12.2	0.057[g]	−7.78[g]	NA	6.1[g]	−1.4	51	82

[a] Data for 5-month (March 23, 1995–August 23, 1995) and 12-month (March 23, 1995–March 26, 1996) elapsed time intervals adapted from Cravotta and Trahan (1999). Data for 60-month (March 23, 1995–March 29, 2000) interval this report (C. A. Cravotta, unpublished data).

[b] Longitudinal distance downflow in meters: 0 is at inflow, 6.1 m is one-fourth distance from inflow to outflow, and 12.2 m is one-half distance from inflow to outflow.

[c] Dissolution rate in units of (g/g/year) normalized by sample surface area to units of (mmol/cm^2/s). Generally, for the Orchard Drift limestone drain, rates normalized by surface area can be computed by dividing k by $10^{6.501}$, which is the product of the average specific surface area of 75 immersed limestone samples (A_{SP} = 1.004 cm^2/g), the millimolar mass of $CaCO_3$(m_{CaCO_3} = 0.1004 g/mmol), and $10^{7.50}$ s/year.

[d] Net concentration of Ca computed as difference between averages for effluent and influent, multiplied by 2.5.

[e] NA, not available. Limestone slabs suspended from tether (noose) at inflow (0-m distance) for a 12-month period dissolved extensively and fell from tether.

[f] Encrustation quantities reported for the 12-month interval should be interpreted with caution because of substantial losses of loosely bound coatings from samples during sample retrieval. Composition of crust that could be salvaged was reported by Cravotta and Trahan (1999).

[g] Due to larger-diameter pipes installed at the inflow to each drain in 1998 (to reduce clogging), flow rates through OLDs actually were increased and, hence, pH near midflow actually was lower during the period 1998 to 2000 than in the preceding years. However, the grand average for pH at the midflow does notreflect this change; the average pH is weighted by more frequent sampling during the first year of operation than during later periods.

undersaturated in the synthetic AMD at near-neutral pH. A similar trend of calcite undersaturation in the Orchard OLD is indicated by the asymptotic, marginal increase in $SI_{CALCITE}$ with increased distance or detention time (Fig. 6A). Slow field dissolution rates and calcite undersaturation could be caused by the precipitation or adsorption of inhibiting agents, which effectively reduce the exposed surface area. The occurrence and possible roles of microbial films and precipitated minerals as inhibiting agents for limestone dissolution have been documented for ALDs and OLDs (Robbins *et al.*, 1996, 1997, 1999). Furthermore, Mg^{2+} and SO_4^{2-}, which are common ions in mine drainage, have been reported to be significant inhibitors of $CaCO_3$ dissolution (Morse, 1983).

D. Limestone Drain Longevity and Size

The longevity of a limestone drain is defined loosely in this chapter as the elapsed time when the mass of remaining limestone will no longer produce sufficient alkalinity to meet treatment goals. Given the empirically derived constants, k and k', the initial alkalinity (C_0), and the maximum alkalinity (C_M), which can be determined with cubitainer tests, the decline in limestone mass through time (age) and any associated decline in alkalinity concentration with decreased mass (detention time) of a limestone drain can be computed. Figure 8 shows the results of computations of mass decay and associated alkalinity for the Howe Bridge 1 and Morrison limestone drains using k and k' derived from cubitainer data for the Howe Bridge and Morrison mine discharges (Figs. 3C and 3B). By overlaying observed data for the actual drains and comparing different results obtained using various values for rate constants, k and k', and porosity, ϕ, the utility and sensitivity of the aforementioned equations to simulate the long-term performance of the limestone drains at these sites can be evaluated.

The projected change in mass of limestone with age of the Howe Bridge 1 and Morrison limestone drains is shown as Fig. 8A. This projection assumes continuous, exponential decay in accordance with Eq. (14) and utilizes the initial mass when constructed (Table I) and the mass-flux decay constant, k, derived from generalized cubitainer data (Fig. 3C). The decay trends are remarkably similar if decay constants derived on the basis of long-term averages for field data are used (dashed curves) because these estimates for k were equivalent to those derived from cubitainer test data. Figure 8B shows the corresponding change in detention time with age as the mass of limestone declines in accordance with Eq. (6). The computed detention time assumes constant flow rate and porosity; detention time decreases if porosity is decreased from 0.49 (solid curves) to lower values (dashed curves).

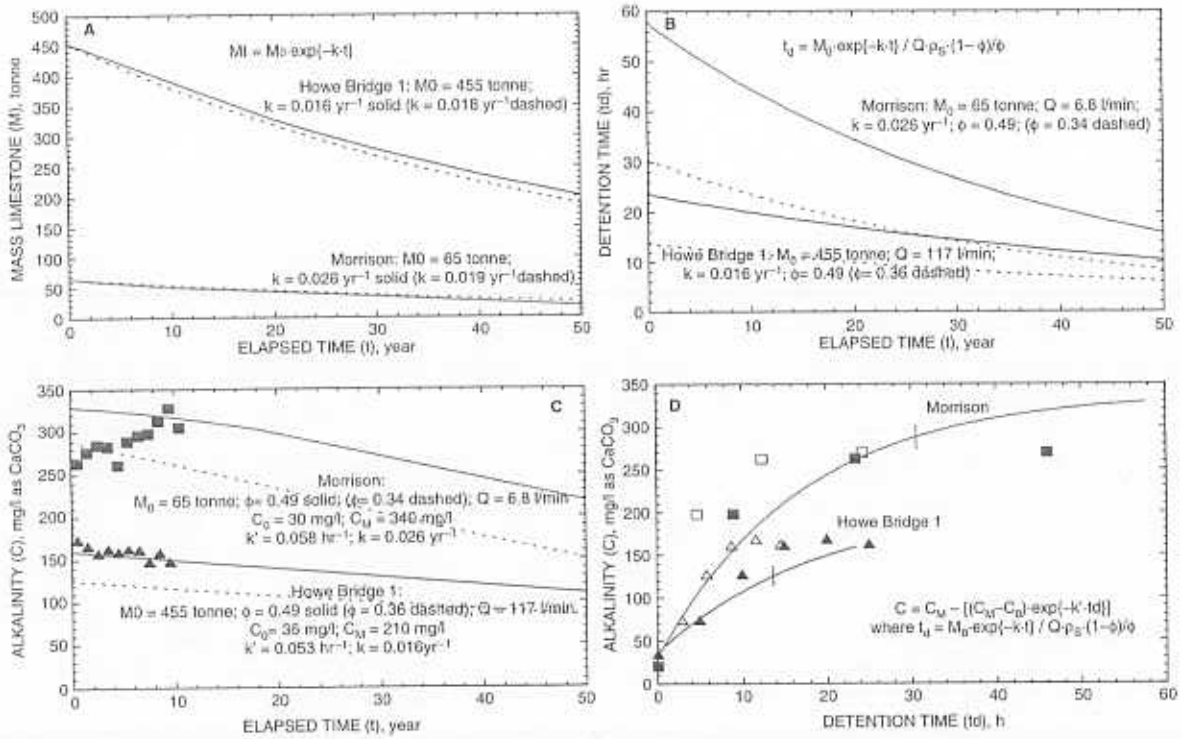

Figure 8 Simulated change in limestone mass, detention time, and alkalinity concentration with age of Howe Bridge 1 and Morrison limestone drains. (A) Mass versus age considering exponential decay and rate constants derived from cubitainer tests (solid) and field flux estimates (dashed). (B) Detention time versus age assuming constant particle density ($\rho_S = 2650\,kg/m^3$), flow rate (Q), porosity = 0.49 (solid), and computed porosity (dashed). (C and D) Simulated (lines) and sampled (points) alkalinity versus age or detention time. Data in C are annual averages for effluent and in D are typical values along longitudinal profile. Solid lines in C and D for porosity = 0.49. Dashed lines in C and open symbols in D are for computed porosity at the respective site.

Figure 8C shows long-term trends for computed and observed alkalinity of effluent from the Howe Bridge 1 and Morrison limestone drains. The simulated alkalinity was computed in accordance with Eq. (10) for progressively declining detention times. The alkalinity simulations (solid curves) used generalized cubitainer data for C_0, C_M, and k' for the respective sites (Figs. 3A, 3B, and 3C). The observed annual average alkalinity of effluent from each of the drains is overlain on the curves. To provide the same baseline influent alkalinity to compare simulated and observed data, the observed values were normalized as the difference between the annual averages for effluent and influent added to the grand average influent concentration. A reasonable match between simulated and observed values for alkalinity is obtained for a porosity of 0.49 at the Howe Bridge site. The lower estimates of porosity based on reported dimensions and mass (Table I) increase the deviation between simulated and observed data trends (dashed lines). However, the simulated and observed trends for the Morrison limestone drain are not closely matched. The Howe Bridge functions as a piston or plug-flow system, with untreated water piped into the limestone drain and detention time of treated water increasing along the length of the drain. In contrast, the Morrison drain intercepts several seeps along its length and hence the effluent is a mixture of water having various detention times. Furthermore, the influent sample for the Morrison drain is collected from an adjacent seep. The sampled seep may not be representative of all the various seeps into the drain.

Figure 8D shows simulated and observed trends for alkalinity with detention time. For the simulations, the greatest detention time for each of the limestone drains is associated with the intial condition (age = 0); detention time and corresponding alkalinity values decrease with increased age. To extend the simulated curves to small detention times at the outflow, the remaining mass and corresponding values for detention time and alkalinity were computed over an elapsed time of 200 years. The resultant estimates for effluent alkalinity after 200 years of continous dissolution correspond with current conditions near the inflow to the drains. Field data for longitudinal samples from monitoring wells within the drains are plotted as individual points in Fig. 8D for comparison with the simulated curves. Assuming a porosity of 0.49, the simulated trend on the basis of the cubitainer tests for the Howe Bridge 1 site matches the observed data for this site. The simulated and observed trends for the Morrison site are not closely matched.

Hedin and Watzlaf (1994) evaluated construction characteristics, detention times, and chemistry of influent and effluent of more than 20 limestone drains to determine the optimum size for maximum alkalinity production. They derived a limestone drain-sizing equation that included a term for longevity and a term for detention time:

$$M = Q \cdot [(t_L \cdot C_M / X_{CaCO_3}) + (t_d \cdot \rho_B \cdot / \phi)], \quad (17)$$

where t_L is the desired longevity of treatment and $\rho_B = \rho_S \cdot (1 - \phi)$ per Eq. (4). With Eq. (17) Hedin and Watzlaf (1994) and Hedin *et al.* (1994a,b) wanted to ensure that the limestone mass computed was sufficient to produce a constant, maximum alkalinity until the specified longevity had elapsed. They solved Eq. (17) for longevity of 20 years and a detention time of 15 h. However, Eq. (17) has several limitations. The first term assumes linear decay (constant mass flux), which is inconsistent with expected exponential decay (Fig. 7), and the second term assumes alkalinity concentration would be constant (maximum) over the effective lifetime of the drain (longevity), after which the remaining limestone mass would be less than that required to produce the specified detention time and alkalinity. The assumption of constant, maximum alkalinity for long detention times (>48 h) is supported by data obtained using cubitainer tests and, to some extent, field data (e.g., Figs. 2 and 4). However, at shorter detention times, alkalinity can vary as a function of influent chemistry, detention time, and/or mass of limestone remaining (Figs. 2, 4, and 8). For large flows that have relatively low net acidity, but still require treatment, the aforementioned approach would indicate excessively large quantities of limestone and large space required for installation.

Alternatively, the size of limestone drains could be estimated using the previously described equations for the exponential decay of limestone and the corresponding alkalinity as a function of detention time (Figs. 3, 7, and 8). The application of these equations requires knowledge of the same variables as Eq. (17) plus the rate constants, k and k', and the initial concentration of alkalinity or Ca of the influent. For example, one may define longevity as the time when the remaining mass of limestone equals that required to achieve a minimum detention time in a drain, such as 15 h that is typically recommended (Hedin and Watzlaf, 1994; Hedin *et al.*, 1994a,b; Watzlaf *et al.*, 2000a). For this computation, Eq. (14) can be rearranged to estimate the elapsed time (t), or age, when the future mass of limestone (M_t) will provide a minimum detention time:

$$t = \ln (M_0/M_t)/k \quad (18)$$

and substituting $M_t = Q \cdot [t_d \cdot \rho_S \cdot (1 - \phi)/\phi]$ per Eq. (7)

$$t = \ln [M_0/(Q \cdot [t_d \cdot \rho_S \cdot (1 - \phi)/\phi])]/k. \quad (19)$$

Equation (19) can be rearranged and solved for the initial mass of limestone that will be necessary to achieve a desired future detention time:

$$M_0 = \exp \{k \cdot t\} \cdot [Q \cdot t_d \cdot \rho_S \cdot (1 - \phi)/\phi] \quad (20)$$

For example, Fig. 9 shows the computed initial mass of limestone to achieve a range of future desired detention times and, hence the alkalinity of effluent per Eq. (10), after an elapsed time of 20 years. Results are shown for constant particle density, porosity, and flow rate and a range of dissolution rates as determined for the 13 limestone drains evaluated. To compute alkalinity as a function of detention time, $k' = 0.053\,h^{-1}$ was assumed on the basis of cubitainer tests for Howe Bridge (Figs. 3B and 6D). Generally, for the application of Eqs. (20) and (10), site-specific data should be used to determine the rate constants, k and k', and the influent and maximum alkalinity or Ca concentrations, C_0 and C_M. Use of larger values for k and/or smaller values for k' will indicate a larger mass requirement and vice versa.

Several factors could account for the observed decreases in alkalinity production rates and computed limestone dissolution rates with age of the limestone drain(s). Review of long-term data indicated no significant trend in the pH or alkalinity of the untreated AMD at the Orchard or Howe Bridge 1 sites, hence the untreated AMD did not become less aggressive with respect to calcite. The decreased rate of dissolution must have been caused by decreased contact between the water and the rock and/or changes in the limestone surface properties. As the limestone mass declines, the exposed surface area will also decline due to (1) rapid dissolution of erodible edges and exposed defects, (2) a smaller total surface area associated with smaller particles or shrunken cores of unweathered limestone, and (3) the accumulation of various minerals and biofilms on the surface. For example, limestone and calcite samples, which were immersed at the inflow and at downflow points within the Orchard OLD, showed effects of both precipitation and dissolution, particularly near the inflow (Cravotta and Trahan, 1999; Robbins *et al.*, 1999). Microscopic examination of calcite mounts on glass slides showed newly formed Fe and Mn oxide and dissolution etch pits (Robbins *et al.*, 1999). The appearance of these secondary minerals in the etch pits implies that sites of dissolution locally could be rendered inactive. Furthermore, the accumulation of large quantities of hydrous oxides or other secondary minerals between limestone fragments, particularly at the bottom of the drain, could reduce the flow of water and contact between the water and limestone through that zone of the limestone drain. This scenario could explain the greater decline in the limestone dissolution rate at the Orchard OLD compared to the Howe Bridge ALD.

E. Attenuation of Acidity and Dissolved Metals

The goal of AMD treatment is to attenuate acidity and metals transport, generally by promoting the formation of solids that can be safely retained on site or disposed. However, metals that accumulate and cannot be flushed

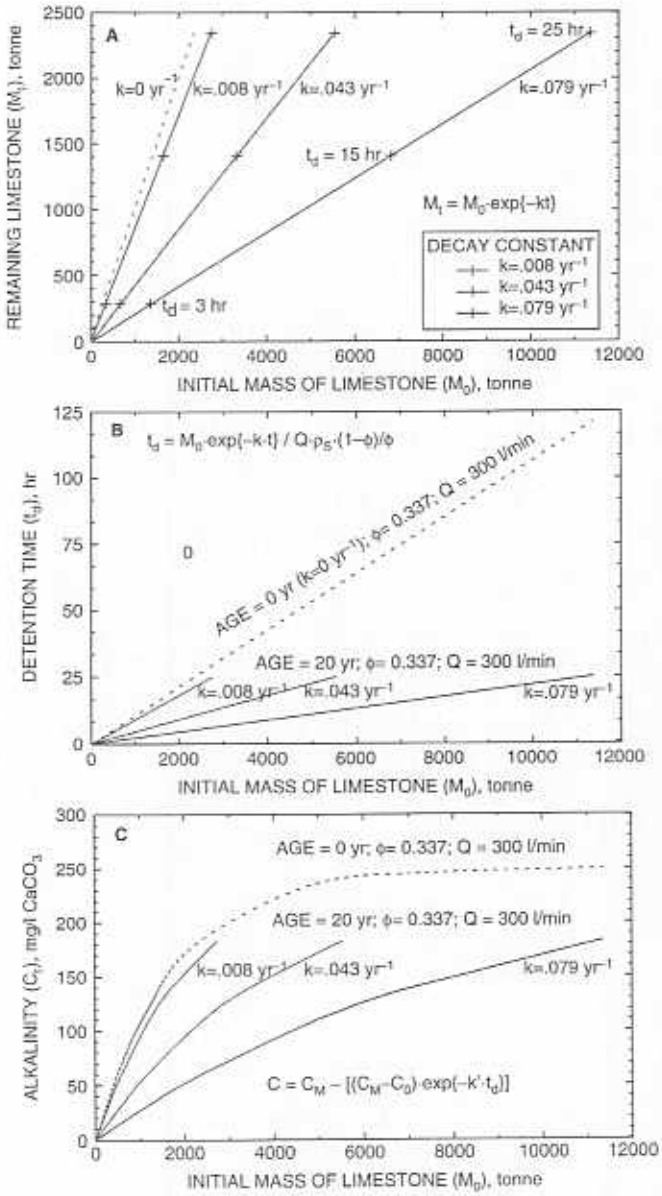

Figure 9 Predictions at 20 years elapsed time of continuous dissolution of an initial mass of limestone, assuming exponential decay at various rates: (A) mass remaining (M_t); (B) detention time (t_d); and C, alkalinity (C_t). Detention time estimated for porosity of 0.337 and flow rate of 300 liter/min. Alkalinity estimated for $C_0 = 0$, $C_M = 250$ mg/liter as $CaCO_3$, and $k' = 0.053\ h^{-1}$.

from a limestone drain or other porous reactive barrier can cause its failure due to the reduction of porosity and/or reduction of limestone surface area. Although the effect on alkalinity production due to reductions in porosity and detention time generally could be evaluated using the aforementioned equations, specific effects on limestone dissolution and alkalinity production rates require additional study.

All 13 of the limestone drain treatments reduced acidity (Table II). The reduction of acidity resulted from the increased pH and alkalinity and associated decreased concentrations of dissolved, readily hydrolyzable metals, including Al^{3+}, Fe^{3+}, and possibly Mn^{2+}, Fe^{2+}, and other divalent cations (e.g., Hedin *et al.*, 1994a; Rose and Cravotta, 1998).

All 13 drains considered for this chapter removed a substantial fraction of Al^{3+} in their influent (Table II). Decreased Al concentration with increased pH is consistent with its solubility control by Al-hydroxide and/or hydroxysulfate minerals (e.g., Nordstrom, 1982; Nordstrom and Ball, 1986). For example, as pH increased within the Orchard OLD, concentrations of Al declined (Fig. 5), whereas equilibrium with poorly crystalline $Al(OH)_3$ was maintained (Fig. 6D). Although the concentration and flux of Al at the Orchard drain were relatively small, where the flux of Al is large, clogging and failure of the drain due to the accumulation of precipitated Al can be rapid, occurring within months (Robbins *et al.*, 1999). The Jennings limestone drain and several others that were constructed to treat low pH, high Al (>5 mg/liter) influent have failed prematurely, primarily due to the precipitation of Al minerals within pores of the drains (Watzlaf *et al.*, 1994, 2000a; Robbins *et al.*, 1996). Although little information is available about the mineralogy of precipitated Al minerals within limestone drains, the formation of Al hydroxysulfate compounds is suspected to be the primary cause of fouling. Generally, Al hydroxysulfate minerals can form when AMD containing dissolved Al^{3+} and SO_4^{2-} attains pH > 4.3 by reaction with limestone or by mixing with near-neutral waters (Nordstrom, 1982; Nordstrom and Ball, 1986; Sterner *et al.*, 1998). For example, Robbins *et al.* (1996) determined an ALD in West Virginia was clogged by poorly crystalline aluminite [$Al_2(SO_4)(OH)_4 \cdot 7H_2O$] and silica. Robbins *et al.* (1999) showed that the Al hydroxysulfate can precipitate within calcite etch pits, interfering with dissolution, and suggested that these compounds can foul limestone drains because of their strong adhesion and high density compared to $Al(OH)_3$. Perforated pipes may not be adequate to flush Al hydroxysulfate minerals from drain pores because of their adhesive nature.

Although dissolved Fe in the influent to all 13 drains was predominantly Fe^{2+}, the influent at several sites also contained Fe^{3+} and/or dissolved O_2. Where anoxic conditions were maintained, Fe concentrations were not

affected by the limestone treatments (Table II).[2] On the basis of equilibrium calculations, Hedin and Watzlaf (1994) suggested that siderite ($FeCO_3$) may have formed in some ALDs; however, the presence of siderite and the significance of Fe^{2+} removal by this mechanism have not been evaluated. Nevertheless, because stoichiometric oxidation of 1 mol of Fe^{2+} requires only 0.25 mol of O_2 (1 mg/liter O_2 for 7 mg/liter Fe^{2+}), losses of dissolved Fe^{3+} *and* Fe^{2+} within OLDs and some ALDs could result from the precipitation of Fe(III) hydroxide or hydroxysulfate minerals, such as ferrihydrite or schwertmannite (e.g., Bigham *et al.*, 1996; Cravotta and Trahan, 1999). The precipitation of Fe(III) compounds implies that O_2 and/or Fe^{3+} enters the drains at the inflow or elsewhere. The Orchard OLD contained 1–3 mg/liter dissolved O_2; despite undersaturation with siderite, Cravotta and Trahan (1999) reported complete removal of Fe^{2+} and Fe^{3+} (Figs. 5B, 5D, and 6C). The attenuation of Fe^{2+} was more efficient than expected on the basis of homogeneous oxidation and precipitation of $Fe(OH)_3$ (Williamson *et al.*, 1992; Kirby and Elder Brady, 1999). Hence, Cravotta and Trahan (1999) attributed the removal of Fe^{2+} to sorption and catalysis of oxidation by $Fe(OH)_3$ (e.g., Tamura *et al.*, 1976; Stumm and Sulzberger, 1992). Microorganisms that could catalyze the oxidation of Fe^{2+} and formation of $Fe(OH)_3$ are ubiquitous in AMD (e.g., Ferris *et al.*, 1989; Ehrlich, 1990; Robbins *et al.*, 1999).

Generally, on the basis of the average composition of influent and effluent, significant removal of Mn and other trace metals was not apparent for the drains evaluated (Table II). Nevertheless, the averages may not represent actual performace through time. For example, Cravotta and Trahan (1999) reported significant removal of Mn, Zn, Ni, and Co within the Orchard OLD after the first 6 months of operation (Figs. 10B and 10C). The hydrous-oxide precipitate that accumulated within the limestone bed had concentrations of Mn, Cu, Ni, and Zn that increased relative to Fe with distance downflow, hence with increased pH. Ratios of Mn/Fe and Mn/Al in the coatings increased by 2 orders of magnitude during the second 6-month monitoring interval relative to the first 6 months (Cravotta and Trahan, 1999). Watzlaf (1997) and Brandt and Ziemkiewicz (1997) also reported substantial Mn removal from AMD by limestone that had been coated by hydrous oxides after a time lag.

The removal of dissolved Mn, Zn, Ni, and Co from solution and a corresponding enrichment of the trace metals relative to Fe in particles and

[2]Apparent decreases in acidity, metals, and SO_4 concentrations in effluent relative to influent at Morrison, Schnepp, and REM-R sites (Table II) should be interpreted with caution because data for nearby seepage were used to represent the "influent" to the Morrison drain and historical data for the untreated AMD were used to represent the "influent" to the Schnepp and REM-R drains. Adjacent seeps rarely have identical chemistry, and water quality of untreated AMD generally improves with time (e.g., Wood, 1996).

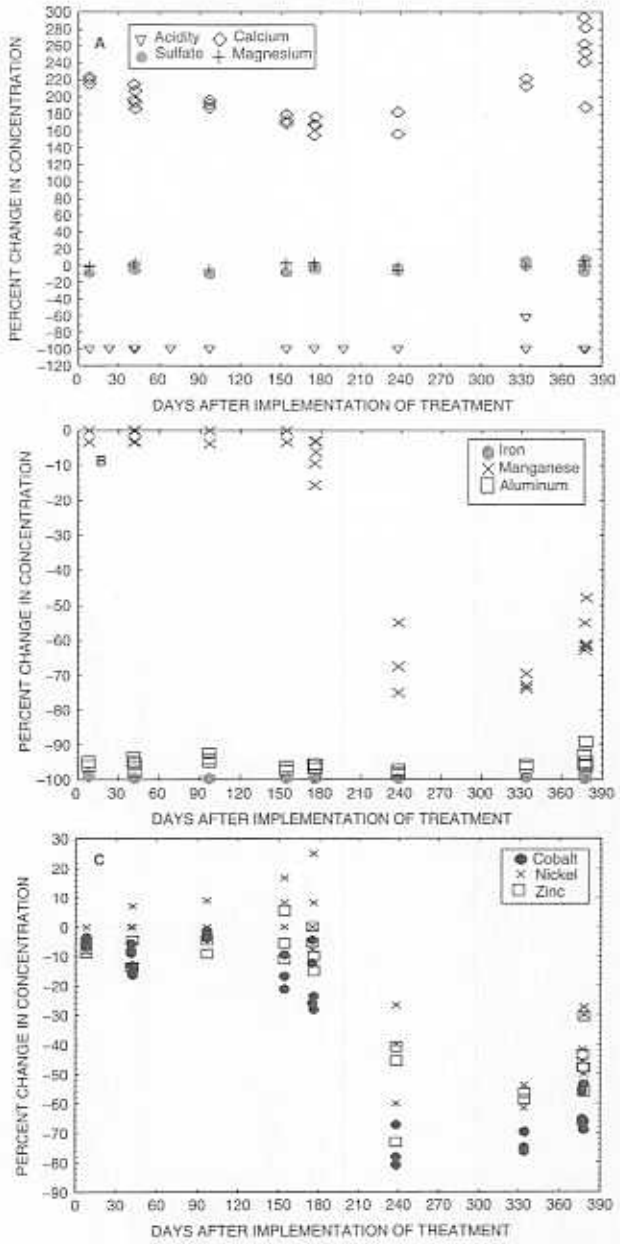

Figure 10 Temporal changes in composition of effluent relative to influent (effluent–influent) at Orchard limestone drain (after Cravotta and Trahan, 1999). Data for samples collected March 1995–March 1996 from Orchard site. From Cravotta and Trahan (1999).

coatings on limestone within the Orchard OLD resulted from sorption and coprecipitation reactions with the hydrous oxides of Fe(III), Mn(II–IV), and, to a lesser extent, Al (Cravotta and Trahan, 1999). Sorption of the trace metals generally can be enhanced by the incorporation of sulfate with hydrous Fe(III) oxides, where the sulfate can be part of the crystal lattice, as with schwertmannite (Bigham *et al.*, 1996; Webster *et al.*, 1998), or can be adsorbed, as with goethite or ferrihydrite (Ali and Dzombak, 1996; Rose and Ghazi, 1997). Uncoated limestone (calcite) generally is not an effective sorbent of the trace metals at pH < 7 (Zachara *et al.*, 1991). Similar trends have been reported for dissolved Mn^{2+} and trace metals to adsorb to hydrous Fe, Al, and Mn oxides, except that the Mn oxides are generally more effective sorbents at lower pH than Fe or Al oxides (Loganathan and Burau, 1973; McKenzie, 1980). Decreases in concentrations of both Al^{3+} and Zn^{2+} through many limestone drains (Table II) imply that some Zn^{2+} could be removed by sorption to $Al(OH)_3$ (e.g., Coston *et al.*, 1995).

The downgradient trends in pH and solute concentrations at the Orchard OLD became progressively more complex through time, particularly near the inflow (Fig. 5), and indicated deviation from piston-flow transport implied for the estimation of detention time as a function of distance downflow within the drain. The complex trends with respect to distance probably resulted from the localized dissolution of limestone and accumulation of hydrous oxides near the inflow that changed the porosity distribution and promoted the development of preferential flow paths. Thus, in addition to the predominant downflow transport and dispersion of hydrous oxide particles away from the inflow, turbulence could have promoted eddying and the recirculation of fluid and suspended particles locally toward the inflow. Similarly, complex trends and explanations for bromide tracer transport through the Howe Bridge 1 and Morrison ALDs were reported by Watzlaf *et al.* (2000a).

Although amorphous to crystalline Fe, Mn, and Al oxides had formed in the Orchard OLD, none of these phases was strongly adhesive. Nevertheless, the Orchard OLD was not equipped with a perforated pipe or other flushing system to prevent the accumulation of solids. However, some solids could be removed in slugs by backflushing, whereby the outflow was closed, causing the hydraulic head to increase inside the drains, and then opened. Hydrous Fe oxides were visible as loosely bound, rust-colored coatings on limestone samples near the inflow and as a gelatinous rusty floc in water samples. After 2 years of operation, numerous black flakes were also visible with the rusty floc. The mixed solids were enriched in Fe (Fe > Al > S = Si > Mn) and contained predominantly schwertmannite and goethite. The black flakes were enriched in Mn (Mn > Fe = Ca > Al) and contained todorokite $[(Ca_{0.393}Mg_{0.473}Mn^{II}_{1.134})Mn^{III}{}_5O_{12} \cdot 2H_2O]$. Although equilibrium computations indicated undersaturation with pure solid phases of Mn(II–IV) and

trace metals, formation of Mn oxides within the OLD may have been favored by near-neutral pH adjacent to limestone surfaces (Cravotta and Trahan, 1999; Robbins *et al.*, 1999). At pH $\geq$6, negatively charged surfaces of the $Fe(OH)_3$ and Mn oxides tend to attract cations, including Fe^{2+} and Mn^{2+}, which can be oxidized rapidly in an aerobic system (Tamura *et al.*, 1976; Hem, 1977, 1978). A variety of microorganisms could have promoted the oxidation of Fe and Mn in the OLD (Ehrlich, 1990; Robbins *et al.*, 1992, 1999). Despite significant concentrations of Al in the solids, the identities of crystalline Al phases could not be determined. Amorphous to poorly crystalline phases of Al, Fe, and Mn likely were present (e.g., Figs. 6C and 6D).

F. Design Considerations for Limestone Drains

The porosity and/or exposed limestone surface area and the flow rate and detention time for water in limestone drains are critical factors affecting their performance because of kinetic controls on dissolution, precipitation, and sorption reactions that control pH and dissolved ion concentrations. For a given flow rate and mass of limestone, detention time will increase with increased porosity; higher porosity can be achieved for uniform, large particles than for mixed size particles. Other factors being the same, alkalinity will increase with increased detention time. Hence, the limestone drain-sizing equation of Hedin and Watzlaf (1994) and Hedin *et al.* (1994a,b) [Eq. (17)] included porosity and detention time as specific variables; however, their equation assumes constant $CaCO_3$ flux and alkalinity over the specified lifetime of the drain. The exponential decay equations introduced in this chapter [Eqs. (10), (14), and (20)] incorporate the same variables as Eq. (17), but also account for corresponding decreases in limestone mass and alkalinity production rates over time on the basis of empirically derived $CaCO_3$ flux data and rate constants. As applied herein, Eqs. (10), (14), and (20) may be useful to extrapolate performance and/or determine the appropriate initial mass required for limestone beds. Their solution was simplified assuming constant rates of limestone dissolution and constant values for flow rate, porosity, and stone density.

The example computations did not consider variations in dissolution rate with water quality along the flow path nor other important chemical processes, such as the precipitation of secondary minerals. The precipitation and dissolution processes can affect the porosity distribution and/or the exposed surface area of the limestone bed. Generally, the formation of secondary minerals and the corresponding reduction of limestone surface area are likely to be associated with influent that does not meet criteria for an ALD (O_2, Fe^{3+}, or $Al^{3+} < 1$ mg/liter). Hence, the exponential equations [Eqs.

(10), (14), and (20)] using short-term test data would be applicable to estimate the mass of an ALD. Before their application for design of an OLD, additional tests may be appropriate. To evaluate mineral coatings on rate constants, parallel tests could be conducted with limestone that is uncoated and identical fragments coated with hydrous Fe, Mn, and/or Al oxides. Potential for clogging and/or flushing could also be evaluated considering measurements of porosity, permeability, and solids transport through a packed bed.

If possible, reducing detention time and maintaining calcite undersaturation in a limestone bed should be considered by splitting inflow to several parallel cells or along the length of a cell instead of directing flow through a single, elongate drain with inflow at one end and outflow at the other. For example, the Orchard OLD split inflow into three parallel troughs, and the Buck Mountain ALD intercepted multiple seeps along its length. The computed $CaCO_3$ fluxes and limestone dissolution rates for these drains were the highest among their respective counterpart OLDs and ALDs considered for this chapter (Table III). This multiple inflow or multiple cell arrangement has advantages and disadvantages. Splitting flow and reducing detention time takes advantage of the kinetics of limestone dissolution, where the rate of dissolution is expected to *decrease* with increased pH and alkalinity and where doubling detention time *will not* double alkalinity. Thus, treatment through parallel cells or along the length of a drain should promote greater dissolution and alkalinity production than a single cell or a series of cells containing the same mass of limestone. Furthermore, for two or more parallel cells, treatment can be conducted continuously through part of the system while flushing or other maintenance is conducted on the other part. The primary disadvantage would be that construction would be more complex and would involve greater area to install several trenches and plumbing for multiple cells than for a single cell. For example, to intercept seepage along its length, a continuous liner at the Buck Mountain. ALD had to be cut into pieces that were installed overlapping like shingles, with the top shingle at the upflow end. Although this arrangement worked to direct influent into and down the drain, it also complicated the monitoring and interpretation of water-quality variations with increased distance or detention time along the drain.

Hedin *et al.* (1994a) advised against the use of horizontally oriented limestone drains for the treatment of AMD containing >1 mg/liter of O_2, Fe^{3+}, or Al^{3+} due to the potential for armoring and clogging of the drains. The presence of any of these constituents can potentially reduce the effective longevity of a limestone drain. However, results of this chapter, combined with results of Watzlaf (1997), Sterner *et al.* (1998), and Cravotta and Trahan (1999), suggest that limestone treatment systems may effectively increase pH and remove dissolved metals, including Mn^{2+}, from AMD

containing moderate concentrations of Fe^{3+} or Al^{3+} (1–5 mg/liter). Caution should be exercised for influent samples that have concentrations near this upper limit because the actual influent composition likely will vary temporally due to droughts, wet periods, and various other environmental factors. Designs should consider these extremes.

Horizontal or downflow systems constructed of coarse limestone could provide sufficient detention times to achieve neutralization of AMD and could be flushed periodically to remove accumulated solids. To enhance trace-metal attenuation by hydrous oxide particles within the drains, the cross section of the drain could be enlarged near the outflow to decrease flow velocities and increase detention time where pH is expected to be highest. To ensure against clogging from an excessive accumulation of hydrous oxides, perforated piping could be installed as subdrains for periodic flushing of excess sludge. Some of these conceptual designs have been constructed but have not been evaluated. For example, at the Hegins drain, valves were installed on perforated laterals that connected to a single longitudinal pipe that was not perforated. This 1-year old system can be flushed, but its long-term performance is uncertain. Additional studies are needed to evaluate such designs and to determine optimum criteria for utilization and construction of limestone drains for AMD remediation. In general, additional information is needed to understand potential for, and effects of, the dissolution of limestone and the formation, accumulation, and transport of secondary metal compounds in AMD treatment systems. Because of the wide range of water chemistry and hydrologic conditions at coal and metal mines (Rose and Cravotta, 1998; Nordstrom and Alpers, 1999), simple to complex remedial alternatives may be appropriate depending on site characteristics.

IV. SUMMARY AND CONCLUSIONS

Although numerous case studies have been reported, published criteria for the construction of limestone drains generally are imprecise and inadequate due to (1) the wide ranges in flow rates and compositions of mine drainage and (2) nonlinear and variable dissolution of limestone and production of alkalinity as functions of water chemistry, detention time, and limestone characteristics. Generally, chemical processes within a limestone drain can be characterized as functions of distance and time as water flows downgradient through the limestone bed. Immediately near the inflow, the pH of the treated water begins to increase as limestone dissolves, ultimately approaching neutrality and calcite saturation, provided that detention time within the drain is sufficient. If treated under anoxic conditions, dissolved

Fe, Mn, and various other metal contaminants such as Co, Ni, and, to a lesser extent, Zn in the AMD tend to be transported conservatively through the drain as pH and alkalinity increase; however, Al tends to be precipitated. Alternatively, if intercepted and treated under oxic conditions, most metals in the AMD can be attenuated by oxidation, precipitation, and/or adsorption processes within the drain. Accumulated metals must be flushed from the drain to prevent clogging, armoring, and failure. Nevertheless, some precipitated materials can be adhesive or encrusting, and hence practically impossible to flush.

The longevity of limestone drains and alkalinity concentration as a function of time can be evaluated as first-order decay, where the remaining mass of limestone at any time is determined as a function of the decay constant, k, and initial mass of limestone [Eqs. (14) and (20)], and the concentration of alkalinity for any detention time is determined as a function of the influent alkalinity, the maximum or steady-state alkalinity, and the rate constant, k' [Eq. (10)]. The application of these equations requires accurate information for the rate constants, porosity, and other variables. Generally, particle density can be assumed constant; however, porosity and bulk density can vary depending on the shape, sorting, and compaction of the particles. For the 13 limestone drains considered in this chapter, computed porosity ranged from 0.12 to 0.50. Computed values for the rate constant, k, ranged from 0.008 to 0.079 $year^{-1}$ on the basis of long-term Ca flux rates. Comparable estimates for k were obtained on the basis of mass lost from immersed limestone samples and short-term cubitainer tests.

Cubitainer testing of the reaction between untreated AMD and limestone intended or available for construction of a limestone drain can provide estimates for maximum alkalinity and the rate constants, k' and k. These data for alkalinity production through time enable determination of the alkalinity concentration that will be produced in treating a specific mine water, the limestone consumption rates, the quantity of limestone needed for a desired design life, and whether the ALD or OLD will produce net alkaline effluent. Because the composition of AMD is a critical factor affecting the alkalinity produced by limestone of a given composition and particle size, cubitainer tests could be conducted repeatedly with different limestone(s) or through time to determine the range of expected conditions within a limestone drain. For an evaluation of mineral coatings on rate constants, tests could be conducted with uncoated limestone and that coated with hydrous Fe, Mn, and/or Al oxides. Potential for clogging and/or flushing should also be evaluated considering measurements of porosity, permeability, and solids transport through a packed bed.

Dimensions and mass of limestone need to be measured accurately to estimate porosity and, ultimately, field detention time. Accurate measure-

ment of flow rate and chemistry of influent and effluent are needed to monitor and evaluate the performance of limestone drains. Additional data for intermediate sampling locations can be useful to evaluate spatial and temporal variations in water chemistry and limestone dissolution. Documentation of hydraulic head at sampling locations could be useful to characterize changes in porosity and permeability distributions within the drain. Variations in porosity within the drain due to the decay of limestone or the precipitation of minerals could be evaluated to refine estimates of detention time and longevity using the equations given previously.

In the Orchard OLD, the rate of limestone dissolution was minimally affected by the accumulation of hydrous Fe, Mn, and/or Al oxides as loosely bound coatings. Despite the ~ 1-mm-thick accumulation of hydrous oxides on limestone surfaces, pH increased most rapidly near the inflow as a result of aggressive dissolution of limestone by the influent AMD. The rate of limestone dissolution decreased with increased pH and concentrations of Ca^{2+} and HCO_3^- and decreased P_{CO_2}. Under the "closed system" conditions in which hydrolysis products including H^+ and CO_2 could not escape the drains and were retained as reactants, limestone surfaces dissolved rapidly, and armoring was avoided, despite oxygenated conditions. However, the computed dissolution rates for the field experiment were about an order of magnitude less than reported laboratory rates at comparable pH. The reason for slower rates of $CaCO_3$ dissolution by AMD (field) than by HCl (laboratory) was not determined but could be due to inhibition of dissolution by Mg^{2+} and/or SO_4^{2-} and potential for various minerals and biofilms to grow on limestone surfaces. Additional studies are needed to determine the hydrochemical conditions and role of microorganisms in mineral precipitation reactions that promote or inhibit limestone dissolution and ultimately can cause failure of limestone treatment systems.

Different conceptual designs for ALDs and OLDs should be considered for promoting the transport of hydrous oxides and optimizing the long-term neutralization of AMD and removal of dissolved metals. For example, splitting inflow to several parallel treatment cells or distributing the influent along the length of a cell should be considered instead of a single, elongate drain with inflow at one end and outflow at the other. This multiple inflow or multiple cell arrangement takes advantage of the kinetics of limestone dissolution, and treatment can be conducted continuously through part of the system while flushing or other maintenance is conducted on another part. Before criteria can be refined for the construction of limestone drains to neutralize AMD, however, various innovative conceptual designs need to be tested, and available data for existing systems need to be evaluated. Long-term performance of OLDs has not been evaluated. Accurate information on variations in the water chemistry, detention time, rates of limestone

dissolution, and effects of hydrolysis products on limestone dissolution, sorption of trace metals, and hydraulic properties is needed to optimize designs for OLDs and ALDs and to minimize costs for the effective implementation of these passive-treatment systems.

ACKNOWLEDGMENTS

The authors gratefully acknowledge long-term, significant contributions of data and interpretations by R. S. Hedin. Other individuals, who are too numerous to name and, in some cases, unknown to the authors, assisted with field work, laboratory analyses, and data compilations used for this chapter. The lead author also belatedly thanks A. C. Lasaga for his enthusiastic efforts at teaching and helpful writing on geochemical kinetics, which formed the basis for the analytical derivations in this chapter. Helpful comments on the early drafts of the manuscript were provided by several colleagues, including R. S. Hedin, R. Runkel, and two anonymous reviewers. However, the interpretations presented are solely the authors' responsibility.

REFERENCES

Ali, M. A., and Dzombak, D. A. (1996). Interactions of copper, organic acids, and sulfate in goethite suspensions. *Geochim. Cosmochim. Acta* **60**, 5045–5053.

Arakaki, T., and Mucci, A. (1995). A continuous and mechanistic representation of calcite reaction-controlled kinetics in dilute solutions at 25°C and 1 Atm total pressure. *Aquat. Geochem.* **1**, 105–130.

Arnold, D. E. (1991). Diversion wells: A low-cost approach to treatment of acid mine drainage. *In* "Proceedings of the 12th Annual West Virginia Surface Mine Drainage Task Force Symposium," pp. 39–50. West Virginia Mining and Reclamation Association, Charleston, WV.

Aschenbach, E. T. (1995). "An Examination of the Processes and Rates of Carbonate Dissolution in an Artificial Acid Mine Drainage Solution." M.S. thesis, Pennsylvania State University, University Park, PA.

Ball, J. W., and Nordstrom, D. K. (1991). User's manual for WAT EQ4F with revised data base: U.S. Geological Survey Open-File Report 91–183.

Bigham, J. M., Schwertmann, U., Traina, S. J., Winland, R. L., and Wolf, M. (1996). Schwertmannite and the chemical modeling of iron in acid sulfate waters. *Geochim. Cosmochim. Acta* **60**, 2111–2121.

Blowes, D. W., and Ptacek, C. J. (1994). Acid-neutralization mechanisms in inactive mine tailings. *In* "Environmental Geochemistry of Sulfide Mine-Wastes" (J. L. Jambor and D. W. Blowes, eds.), Vol. 22, pp. 271–292. Mineralogical Association of Canada, Short Course Handbook.

Brady, K. B. C., Hornberger, R. J., and Fleeger, G. (1998). Influence of geology on post-mining water quality—Northern Appalachian Basin. *In* "Coal Mine Drainage Prediction and Pollution Prevention in Pennsylvania" (K. B. C. Brady, M. W. Smith, and J. Schueck, eds.),